OVATE AND ITS ASSOCIATES:

THE INTERACTIONS OF TOMATO OVATE WITH TRMs AND TON1

by

CARMEN KRAUS

(Under the Direction of Esther van der Knaap)

ABSTRACT

OVATE is highly expressed in young floral organ primordia. Wild tomato nearly isogenic lines with *ovate/sov1* mutations produce pear-shaped fruit. TONNEAU1 Recruiting Motif (TRM) proteins are part of the OVATE FAMILY PROTEIN (OFP)-TRM complex regulating tomato fruit shape, and are part of the TONNEAU1 (TON1), TRM, Phosphatase PP2A (TTP) complex which is involved in the regulation of plant cell division patterns. OVATE-TRM3/4-TON1b protein subcellular localizations were examined in tobacco. When these proteins are co-expressed, they colocalize in the cytosol instead of the microtubules like TRM3/4. Interaction mutants of OVATE and TRM3/4 co-expressed with TON1b also colocalize in the cytosol. OVATE can re-localize the TRM/TON protein complex independent of its interaction with TRM3/4. Young flower buds were examined of *ovate/sov1*, *ovate/sov1/trm5*, and wild type LA1589 accessions. Bud shape differences between the accessions were apparent at 7 days post initiation. These results suggest that *OVATE* affects ovary patterning early in gynoecium development.

INDEX WORDS: OVATE, OFP20 (SOV1), TONNEAU1 Recruiting Motif (TRM), TONNEAU1 (TON1), protein localization, flower bud, tomato, confocal microscopy

OVATE AND ITS ASSOCIATES:

THE INTERACTIONS OF TOMATO OVATE WITH TRMs AND TON1

by

CARMEN KRAUS

BS, University of Georgia, 2015

BFA, University of Georgia, 2015

A Thesis Submitted to the Graduate Faculty of The University of Georgia in Partial Fulfillment of the Requirements for the Degree

MASTER OF SCIENCE

ATHENS, GEORGIA

2019

OVATE AND ITS ASSOCIATES:

THE INTERACTIONS OF TOMATO OVATE WITH TRMs AND TON1

by

CARMEN KRAUS

Major Professor: Esther van der Knaap
Committee: Anish Malladi
Wolfgang Lukowitz

Electronic Version Approved:

Suzanne Barbour
Dean of the Graduate School
The University of Georgia
August 2019

DEDICATION

To the climbing wall, for making me boulder.

ACKNOWLEDGEMENTS

Thanks to Esther van der Knaap for her help and support. I came to her office looking for a lab tech job, and she convinced me to pursue a master's! Thank you for letting me explore a project that let me combine my loves of science and art. And thank you for introducing me to the Athens running clubs!

Thanks to my committee members Wolfgang Lukowitz and Anish Malladi for taking the time to review my thesis and ask such thoughtful questions during my defense.

Thanks to the whole van der Knaap lab for their assistance and friendship. Thanks especially to Neda Keyhaninejad for helping me with the confocal and to Ashley Snouffer for proofreading. Thanks to my fellow graduate students Nathan Taitano, Manoj Sapkota, Yasin Topcu, and Alexis Ramos for being such great friends, and thanks Nathan for the puns and always having my back.

Thanks to my parents for their love and support during my degree (and all the time). Thanks for making food for me and encouraging me to do my best.

Thanks to all my friends, in the department and elsewhere, for being such great people. I am so thankful to have met all of you.

TABLE OF CONTENTS

Page

LIST OF TABLES

Page

LIST OF FIGURES

Page

CHAPTER 1

INTRODUCTION AND LITERATURE REVIEW

Humans are fascinated by fruit shape. Wild fruits are mostly small and round, while cultivated fruits have a variety of shapes. Larger fruit size and different fruit shapes have been selected during the cultivation of many crops, including tomato. Wild type tomato fruits, exemplified by *Solanum pimpinellifolium* accession LA1589, are round and only a centimeter in diameter. Cultivated tomatoes (*Solanum lycopersicum*) come in all shapes and sizes. The cultivated heirloom tomato Yellow Pear is aptly named because its fruits have a distinct pear shape. This eccentric form results from histological changes primarily at the proximal end of the fruit, which make the locules off-center along the proximal-distal axis (van der Knaap et al., 2014).

Tomato is a good model species to understand fleshy fruit growth and development. A few tomato fruit shape genes, namely *SUN, OVATE, SlOFP20* (*SOV1*)*, LC,* and *FAS*, have been cloned thus far (Rodríguez et al., 2011; Wu et al., 2018). This research investigates the interactions of OVATE and SlOFP20 with other proteins that affect plant morphology.

OVATE and the Ovate Family Proteins

Early in the 20th century after the rediscovery of Mendel's Laws about heredity, pear-shaped tomato fruit was shown to be an heritable trait and the locus was called *ovate* (Price and Drinkard, 1909). The locus was mapped on the long arm of

chromosome 2 from a cross of Yellow Pear with LA1589 (Ku et al., 1999). Finemapping and cloning led to the discovery of the gene, which was named *OVATE* after the locus (Ku et al., 2001; Liu et al., 2002). The *ovate* mutation present in pear-shaped fruit like Yellow Pear is a single-nucleotide nonsense mutation in an exon of *OVATE* resulting in a premature stop codon (Liu et al., 2002). A class of proteins shares similarities to OVATE and was named the Ovate Family Proteins (OFPs) (Hackbusch et al., 2005). These proteins share the C-terminal OVATE domain. *OVATE* is primarily expressed in the floral meristem and in young buds (Wu et al., 2018).

Not all tomato cultivars with the *ovate* mutation have pear-shaped fruit, however. This incongruity is due to loci named *suppressor of ovate1* (*sov1*) and *sov2* that result in a range of shapes associated with tomato varieties that carry the *ovate* mutant allele (Rodríguez et al., 2013). The action of the *sov1* locus is due to a promoter mutation in *SlOFP20* that results in reduced gene expression (Wu et al., 2018). *OFP20* is highly expressed at anthesis but has low expression in young buds and in other plant organs. Double mutants of *ovate/sov1* display increased elongation and pear shape in the final fruit as well as the anthesis ovaries. The *ovate*/*sov1* mutations influences cell division at the proximal end of the fruit. The anthesis ovaries of *ovate/sov1* double mutants in the LA1589 background had significantly more cells in the proximal-distal direction and significantly fewer on the medial-lateral axis than the wild type and the single mutants (Figure 1.1) (Wu et al., 2018).

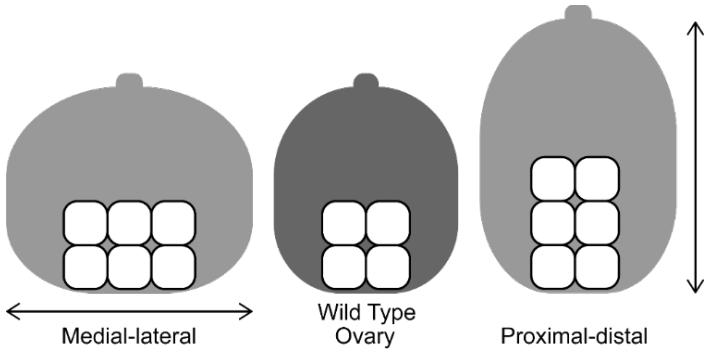

Figure 1.1. Medial-lateral vs. proximal-distal cell division in a tomato ovary.

Even though the gene was identified 17 years ago, little is known about the molecular functions of OVATE and OFPs in plants. The homolog of tomato *OVATE* in Arabidopsis is most likely *AtOFP7* (Huang et al., 2013; Liu et al., 2014). Plants that overexpressed *AtOFP1* had reduced cell elongation and over-expressors of *AtOFP2* and *AtOFP7* also had similar phenotypes (Wang et al., 2007). The most likely ortholog of SlOFP20 in tomato is AtOFP1. Overexpression of *AtOFP1* leads to stunted plants (Hackbusch et al., 2005; Wang et al., 2007). OFPs encode a nuclear localization signal, which would support their influence on development (Liu et al., 2002; Yu et al., 2015). The stunting of the plant organs results from reduced cell elongation (Wang et al., 2007). Most of the research on *AtOFPs* was conducted using overexpression instead of loss-of-function mutations, since the phenotypes of loss-of-function plants were largely unchanged (Li et al., 2011; Wang et al., 2007; Wang et al., 2011). The original hypothesis is that OFPs are transcriptional repressors since these proteins negatively regulate growth and transcriptional repression was observed in luciferase assays (Wang et al., 2007). Recent findings support a role for the family in regulating subcellular localization of protein complexes (Lazzaro et al., 2018; Wu et al., 2018).

Overexpression of OFPs in *Arabidopsis* tend to overwhelm the system and can have ectopic side effects whereas knockout mutations have subtle if any phenotype (Liu et al., 2002; Wang et al., 2007; Wang et al., 2011). In contrast, tomato *ovate* displays an obvious mutant phenotype in its ovary and fruit shape.

Interestingly, OFPs are found in all land plants—and only in land plants—from early-diverged mosses to crops (Liu et al., 2014). There are 19 known OFPs in Arabidopsis and 31 known OFPs in tomato. In Yeast Two-Hybrid screens, nine AtOFPs were associated with Three-Amino Acid Loop Extension (TALE) proteins such as BELL and KNOX (Hackbusch et al., 2005). AtOFPs move TALEs from the nucleus to the cytoplasm and potentially to the cytoskeleton. These AtOFPs showed an extensive interaction network, indicating these proteins are important members of pathways (Hackbusch et al., 2005). AtOFP1 might also affect the Non-Homologous End Joining (NHEJ) pathway and interacted with Ku70/80 (Wang et al., 2010). Additionally, AtOFP4 and AtOFP1 interact with KNOTTED ARABIDOPSIS THALIANA7 (KNAT7), a TALE protein, and BEL-LIKE HOMEODOMAIN6 (BLH6) to negatively regulate the formation of the secondary cell wall (Liu and Douglas, 2015). OsOFP2 in rice interacts with putative KNOX and BELL transcription factors (Schmitz et al., 2015). Additionally, AtOFP5 is associated with TALE proteins BLH1 and KNAT3 in the developmental regulation of egg and synergid cells (Pagnussat et al., 2007). OFPs influence brassinosteroid signaling in rice (Yang et al., 2016) and ripening in banana (Liu et al., 2015). Melon and cucumber fruit shape Quatitative Trait Loci (QTL) intervals contain OFP members, *CmOFP13* and *CsOFP15* respectively (Wu et al., 2018). Additionally, potato contains an ortholog of OFP20 that appears to control tuber shape (Wu et al.,

2018). These diverse roles of OFPs in plants demonstrate the importance of this protein family.

The pre-prophase band (PPB) and TONNEAU1

In non-dividing plant cells, the cortical microtubules are located directly below the plasma membrane. Unlike animal cells, plant cells do not have centrosomes or similar structures to organize microtubules. The microtubule arrays of growing plant cells are perpendicular to the direction of cell growth during interphase. During pre-prophase prior to cell division, the cortical microtubules reorganize to form the pre-prophase band (PPB). This structure predicts the future location of the cell plate and thus the plane of division (Hashimoto, 2015). Plant cells are held in place by their cell walls, so it is important that the cells divide in the correct plane for proper plant growth and development. Disruption of the PPB structure leads to abnormal growth and stunting or embryo lethal phenotypes (Spinner et al., 2010).

Only two *Arabidopsis* mutants that are unable to form a PPB have been identified thus far: *ton1* and *fass*. These mutants display strong stunted phenotypes from abnormal cell division due to their lack of PPB (Azimzadeh et al., 2008). The *TONNEAU1* (*TON1*) locus of *Arabidopsis* has two tandemly arranged genes: *TON1a* and *TON1b*. Only these two members of the *TON1* gene family have been identified and knock out alleles causes extreme phenotypes, indicating that these genes are essential for plant growth. Tomato also has *TON1a* and *TON1b*, although the genes are 40Mb apart. TON1 has similarities to centrosome proteins from humans (Azimzadeh et

al., 2008). Also, like OFPs, TON1 is found in all land plants including mosses (Spinner et al., 2010).

TON1 interacts with microtubules through a regulatory complex comprised of TON1, TONNEAU1 Recruiting Motif (TRM), and protein phosphatase 2A (PP2A) proteins (Spinner et al., 2013). FASS is a regulatory subunit of PP2A (Camilleri et al., 2002). TRM proteins recruit this complex to the microtubules (Spinner et al., 2013). AtTRM1 can target AtTON1 to the microtubules (Drevensek et al., 2012). This TON1/TRM/PP2A (TTP) complex associates with the cortical microtubules and the PPB, indicating its potential importance in organizing the microtubules.

OVATE interacts with members of the TONNEAU1 Recruiting Motif (TRM) proteins

The TRM protein superfamily was first described in *Arabidopsis* (Drevensek et al., 2012). This family is large, with 34 known members in *Arabidopsis* and 26 members in tomato. TRM1 and TRM2 were already known in *Arabidopsis* as LONGIFOLIA2 (LNG2) and LONGIFOLIA1 (LNG1), respectively, and contribute to cell elongation (Lee et al., 2006). Many TRMs, though not all, localize and bind to the cortical microtubules (Drevensek et al., 2012). TRMs can bind to TON1 through their M2 motif, which is conserved across the protein family (Drevensek et al., 2012). SlTRM3/4 and SlTRM5 are the closest homologs in tomato of the AtTRM1-5 clade. This clade is important because it has been shown to regulate the organ shape of leaves and fruits (Wu et al., 2018).

OVATE interacts with 11 of the 26 known tomato TRM proteins in Yeast two-hybrid (Y2H) screens (van der Knaap et al., 2014). The OVATE domain of OFPs

interacts with the TRM M8 motif and coexpression of OVATE with some TRM members results in different localization patterns (Wu et al., 2018). Therefore, OVATE and OFP20 can regulate fruit shape by interacting with the TRMs potentially by influencing the TTP complex recruitment to the microtubules.

OFPs and TRMs are members of large protein families and their mutants display milder knockout phenotypes than TON1. These results indicate that TON1 proteins are essential for plant development but that TRM and OFP protein families have overlapping functions or interact for subtler phenotypic changes. The cytoskeleton is important for cell growth and division so the interaction of OVATE, TRMs, and TON1 should have an impact on fruit growth.

Present study

This thesis is composed of two related studies. The goal of the first study, described in Chapter 2, is to investigate the subcellular localization of OVATE, TON1, and TRM3/4. It tests the hypothesis that OVATE disrupts the recruitment of TON1 by TRMs to the microtubules. The goal of the second study, described in Chapter 3, is to examine how early ovary shape is affected by OVATE and OFP20 (SOV1) by examining early stage tomato flower buds.

Research on OFPs, TRMs, and TON1 could lead to a better understanding of the mechanisms that affect fruit shape. This information could assist vegetable and fruit breeders in the design of shapes targeted to certain market classes or mechanical harvest. For example, pear-shaped tomatoes are agronomically useful because they offer a greater variety of tomato shapes that are easily recognized by consumers.

Additionally, pear shape is genetically interesting because this shape mainly results from elongation of the proximal end of the ovary before anthesis. Elucidation of this mechanism would greatly help understand how fruit develops and why fruits have such diverse shapes. Few fruit shape genes have been cloned so far, so this research is novel. This study is one within a comprehensive line of research conducted in the lab of Dr. Esther van der Knaap. This research is aimed at understanding the mechanisms fruit development and plant growth, which will additionally assist in the development of new and unique cultivars for all vegetable and fruit crops.

CHAPTER 2

OVATE, TON1b, AND TRM3/4 INTERACT IN *NICOTIANA BENTHAMIANA*[1]

[1]Kraus, C.O. and E. van der Knaap. To be submitted to *Plant Biology*.

Abstract

Plant cells tightly regulate the orientation of cell division. TONNEAU1 Recruiting Motif (TRM) proteins are part of the TONNEAU1 (TON1), TRM, Phosphatase PP2A (TTP) complex, which is involved in the regulation of plant cell division patterns. TRMs recruit the TTP to the cortical microtubules and the pre-prophase band. Additionally, TRMs are also part of the OVATE FAMILY PROTEIN (OFP)-TRM complex regulating tomato fruit shape. In this study, the interaction dynamics of OVATE, TON1, and TRM3/4 were investigated as the localization of the three proteins together was unknown. *Agrobacterium* expressing *OVATE*, the mutant *OVATE D280R*, *OFP20*, *TRM3/4*, the mutant *TRM3/4 K560V* and *TON1b* were used to examine localization patterns in *N. benthamiana* epidermal cells. When TRM3/4 and OVATE were co-expressed, they colocalized to the cytosol. TRM3/4 expressed singly and co-expression of TRM3/4 and TON1b both led to localization in the microtubules. When OVATE, TRM3/4, and TON1b were triple expressed, all three proteins colocalized in the cytosol. Mutants that change amino acids within the interacting domains of OVATE and TRM3/4, OVATE D280R and TRM3/4 K560V respectively, interacted much less when expressed together as expected. However, the triple expression of OVATE D280R, TRM3/4 K560V, and TON1b still localized to the cytosol. Additionally, when OFP20, TRM3/4, and TON1b were triple expressed, all three proteins colocalized to the microtubules with OFP20 also showing some nuclear signal. These results support the hypothesis that OVATE can re-localize the TRM/TON protein complex independent of its interaction with TRM3/4, potentially through direct interaction with TON1b. OVATE and OFP20

may differentially regulate the subcellular localization of the TTP complex as seen by their different localization patterns.

Introduction

The plane of plant cell division is important for proper plant growth. Plant cells have ridged cell walls, so the cells are fixed in place. Therefore, the division plane needs to be in the correct orientation for the proper arrangement of cells within a tissue. The direction of cell division is marked by the pre-prophase band (PPB), a collection of the cortical microtubules that forms in the location of the future cell plate and thus the plane of cell division (Hashimoto, 2015). Although a recent study found the PPB is not vital in the division orientation, it does function to ensure directional cell divisions are robust (Schaefer et al., 2017). Plant cells do not have microtubule organizing centers, such as centrosomes that are found in animal cells, but microtubule organization remains essential for orientation of cell divisions (Azimzadeh et al., 2008).

Several known genes, namely *SUN*, *OVATE*, *SlOFP20* (*SOV1*), *LC*, and *FAS,* affect tomato floral meristem, ovary, and fruit development, causing changes in final fruit shape (Rodríguez et al., 2011; van der Knaap et al., 2014; van der Knaap and Østergaard, 2017; Wu et al., 2018). These genes account for the majority of natural variation in tomato fruit shape, but the molecular mechanisms are not well understood. OVATE Family Proteins (OFPs) were initially identified as transcriptional repressors in *Arabidopsis* (Wang et al., 2007; Wang et al., 2011). However, recent research indicates that OVATE and other OFPs function in subcellular localization of proteins (Wu et al., 2018).

OVATE interacts with the M8 motif of members of the TONNEAU1 Recruiting Motif (TRM) family. Of the 26 TRMs in tomato, 11 were identified in a Yeast 2-Hybrid (Y2H) screen with OVATE as the bait (van der Knaap et al., 2014; Wu et al., 2018). Although not all TRMs have the same subcellular localization pattern, tomato TRM5 and TRM3/4 localize exclusively to the microtubules when expressed singly in *Nicotiana benthamiana* (Wu et al., 2018). TRM5 and TRM3/4 are homologs of the AtTRM1-5 subclade, which affects organ shape in *Arabidopsis* (Lee et al., 2006). Members of the TRM protein family target TONNEAU1 (TON1) to the microtubules (Drevensek et al., 2012; Spinner et al., 2013). TON1 is necessary for proper PPB formation and *ton1* mutants have extreme stunted phenotypes in *Arabidopsis* (Azimzadeh et al., 2008). TON1 is part of the TRM-TON-PP2A (TTP) complex, which associates with the cortical microtubules and the PPB (Spinner et al., 2013; Spinner et al., 2010). In Arabidopsis, *TON1* has two members: the tandemly located *TON1a* and *TON1b*. Tomato also has two *TON1a* and *TON1b*, but the genes are 40Mb apart. When AtTON1a or TON1b are singly expressed in *N. benthamiana*, these proteins localize to the cytosol and cytoplasmic strands.

OVATE interacts with TRMs when co-expressed in *N. benthamiana* in addition to interacting in the Y2H screen (Wu et al., 2018). In single expression studies, OVATE localizes to the cytosol. When OVATE is co-expressed with microtubule-associated TRM3/4, OVATE recruits these proteins to the cytosol (Wu et al., 2018). This change in localization of a TRM suggests that OVATE could have a role in regulating the subcellular location of the TTP complex. The OFP domain of OVATE interacts with the TRM M8 motif. When the negative D280 residue in the OFP domain of OVATE and the

positive K560 residue in the M8 motif of TRM3/4 are exchanged for a neutral or opposite charge residue, OVATE interacts less with TRM3/4 (Wu et al., 2018).

OFP20 is also an important member of the OFPs. This gene was identified in tomato as *Suppressor of Ovate 1* (*SOV1*). Double mutants of *ovate/sov1* in the wild tomato background have pear-shaped fruit, a much more extreme phenotype than either the *ovate* or *sov1* mutation by itself (Wu et al., 2018). OFP20 localizes to the nucleus and the cytosol.

The molecular function of OFPs and the significance of their interaction with TRMs remains to be determined. One hypothesis is that OFPs may regulate the subcellular localization of the TTP complex and impact microtubule architecture and cell division orientations to ultimately regulate fruit shape. This study investigates the effect OVATE has on the subcellular localization of different components of the TTP complex and is guided by the hypothesis that OVATE disrupts the recruitment of TON1 by TRMs to the microtubules, thereby impacting the subcellular localization the TTP complex.

Methods

Plasmids used in the experiment

Clones of *OVATE*, *OVATE D280R*, *OFP20*, *TRM3/4*, *TRM3/4 K560V* and *TON1b* made by Shan Wu and Neda Keyhaninejad were used in this experiment. *TON1* has two copies in tomato, *TON1a* and *TON1b*. *TON1b* was used for this experiment instead of *TON1a* because *TON1b* has better expression in *N. benthamiana*. The vectors containing the cloned fragments carry a resistance gene for spectinomycin and were transformed into *Agrobacterium tumefaciens* strain C58C1, which is resistant to

rifampicin and gentamycin. All genes are expressed under the double 35S promoter. To create the mutant OVATE D280R, Keyhaninejad mutated the negatively charged Aspartate (D) residue in the OFP domain of OVATE to a positively charged Arginine (R). To create TRM3/4 K560V she mutated the wild type protein to change the positively charged Lysine (K) residue to a hydrophobic Valine (V).

The *Agrobacterium* were grown from frozen stock stored in glycerol in a -80°C freezer. Colonies were grown on media plates containing 50 µg/ml of gentamycin, 25 µg/ml rifampicin, and 100 µg/ml of spectinomycin. Plates were used for 3 weeks, then a new plate was made from culture or from frozen stock.

Agroinfiltration of Nicotiana benthamiana

Single *Agrobacterium* colonies for each clone were selected and grown overnight in liquid media containing gentamycin, rifampicin, and spectinomycin in a 28°C shaker at 200-250 rpm. The next day, the agrobacterium were pelleted in a centrifuge at 4700 rpm for 17 minutes. An infiltration buffer of 10 mM MgCl2, 10 mM MES and 150 mM acetosyringone was used to resuspend and dilute the Agrobacterium to approximately 0.2-0.3OD. The mixture incubated for 3 hours at room temperature. Equal amounts of the bacterial solution were mixed together for co-expression analysis. For each round of infiltration, single, double, and triple combinations of proteins were made. P19, a suppressor of gene silencing, was added to all single, double, and triple co-expressions except singly expressed TON1b. The bacterial suspension was injected into the underside of the first two to three true leaves of *N. benthamiana* using a 3ml needleless syringe. The plants were grown in a 23°C growth chamber (12-hour day, 24°C) for 48-72 hours prior to microscopy.

Confocal microscopy

Protein localization was viewed at the Biomedical Microscopy Core at the University of Georgia using a Zeiss LSM 880 confocal microscope. Small leaf samples, approximately 1 mm x 1 mm, were cut and mounted in water on a glass slide for viewing in the microscope. The singly expressed proteins were checked for good signal, and cells from the plants with the triple and double expressed proteins were counted. The localization of the proteins was scored as cytosol, microtubules, and/or nucleus. To count the cells, well-expressing cells were identified using the eyepieces at 40x magnification. If the cell seemed to have good expression for all constructs, it was further analyzed on the computer to score localization visually. Cells were scored for location by color channel. As many cells as possible were counted per leaf sample. For co-expression of OVATE-TRM3/4-TON1b, three independent replicates were used. For co-expression of OVATE D280R-TRM3/4 K560V-TON1b, four independent replicates were used. For co-expression of OFP20-TRM3/4-TON1b, three plants infiltrated on the same day were combined.

Results

OVATE and TRM3/4 colocalize in the cytosol, but this interaction is disrupted for the OVATE D280R and TRM3/4 K560V mutants

When singly expressed in *N. benthamiana*, OVATE and OVATE D280R localized to the cytosol, and TRM3/4 and TRM3/4 K560V localized to the microtubules (Table 2.1, Figure 2.1a). When OVATE and TRM3/4 were co-expressed, both proteins colocalized in the cytosol (Figure 2.1b). This result was observed for 100% of cells counted (n=57)

and confirms previous findings (Figure 2.2a). The OFP domain of OVATE interacts with the M8 motif of TRM3/4. When the OVATE D280R and TRM3/4 K560V mutants were co-expressed in *N. benthamiana*, 100% of OVATE D280R remained in the cytosol and 82% of TRM3/4 K560V had returned to the microtubules (n=44, Figure 2.2b, Figure 2.1d). This result also confirms previous findings.

Table 2.1. Clones used for agroinfiltration with their fluorescent tag and localization when expressed singly.

Gene	Fluorescence	Localization
OVATE	RFP	Cytosol
OVATE D280R	RFP	Cytosol
OFP20	GFP	Nucleus and Cytosol
TRM3/4	GFP, RFP	Microtubules
TRM3/4 K560V	GFP	Microtubules
TON1b	CFP	Cytosol

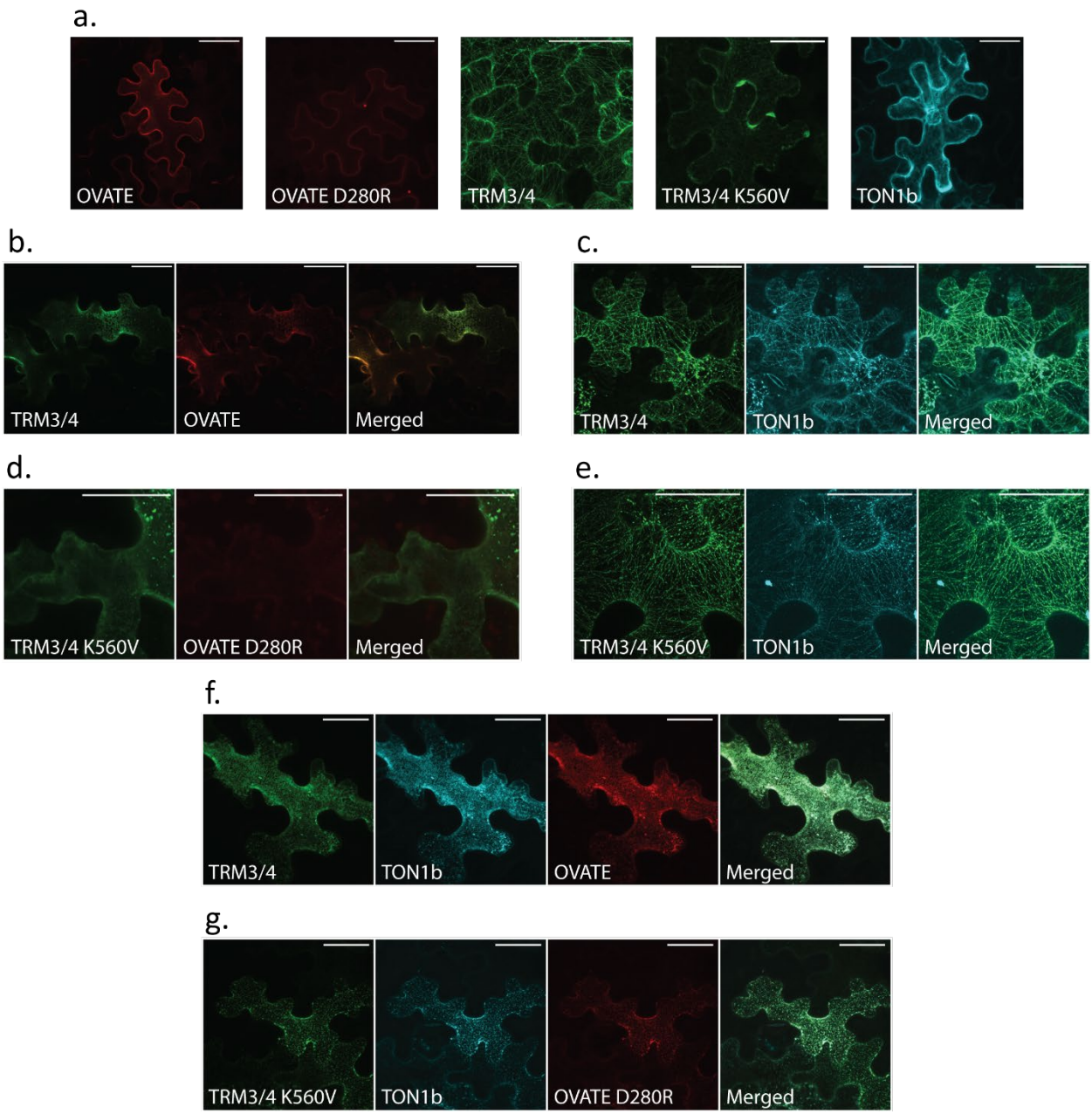

Figure 2.1. Subcellular localization patterns of a) singly expressed proteins, b) double expressed TRM3/4 + OVATE, c) double expressed TRM3/4 + TON1b, d) double expressed TRM3/4 K560V + OVATE D280R, e) double expressed TRM3/4 K560V + TON1b, f) triple expressed TRM3/4 + TON1b + OVATE, and g) triple expressed TRM3/4 K560V + TON1b + OVATE. Bars are 50 μm.

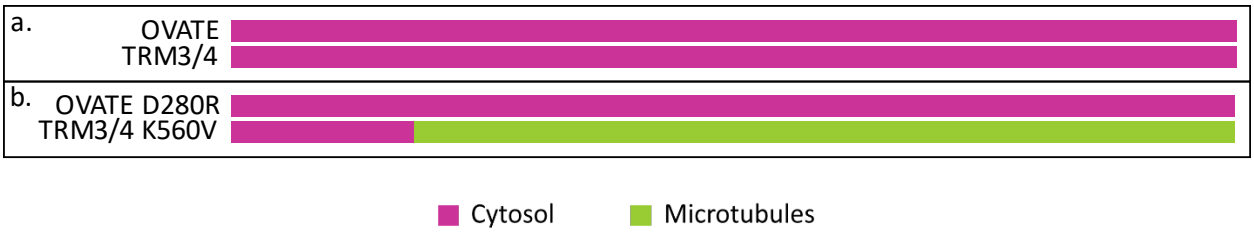

Figure 2.2. Percentage of counted cells with proteins localizing to either the cytosol or microtubules for double expressions of a) OVATE + TRM3/4, n=57 and b) OVATE D280R + TRM3/4 K560V, n=44.

TRM3/4 and TON1b colocalize in the microtubules, and this interaction remains intact with the TRM3/4 K560V mutants

When singly expressed in *N. benthamiana*, TRM3/4 and TRM3/4 K560V localized to the microtubules and TON1b localized to the cytosol and cytosolic strands (Table 2.1, Figure 2.1a). When TRM3/4 and TON1b were co-expressed in *N. benthamiana*, TRM3/4 recruited TON1b to the microtubules. Microtubule signal was seen in 100% of TRM3/4 cells and 97% of TON1b cells (n=31, Figure 2.3a, Figure 2.1c). This result confirms previous studies. TON1b interacts with the TRM3/4 M2 motif, thus the TRM3/4 K560V mutation should not affect their colocalization. Indeed, when TRM3/4 K560V and TON1b were co-expressed cells had 100% microtubule signal for TRM3/4 K560V and 96% microtubule signal for TON1b (n=31, Figure 2.3b, Figure 2.1e).

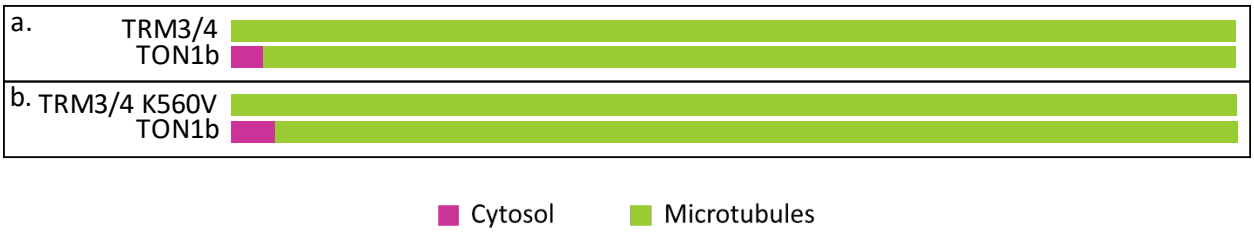

Figure 2.3. Percentage of counted cells with proteins localizing to either the cytosol or microtubules for double expressions of a) TRM3/4 + TON1b, n=31 and b) TRM3/4 K560V + TON1b, n=46.

OVATE, TON1b, and TRM3/4 localize in the cytosol when co-expressed

Singly expressed, OVATE proteins localized in the cytosol, TON1b proteins localized to the cytosol and cytosolic strands, and TRM3/4 proteins localized to the microtubules (Table 2.1, Figure 2.1a). When TON1b and TRM3/4 were co-expressed, the proteins colocalized to the microtubules. However, when TRM3/4 and OVATE were co-expressed, the proteins colocalized to the cytosol. Triple expressed constructs of OVATE, TON1b, and TRM3/4 in *N. benthamiana* colocalized in the cytosol. OVATE cytosol signal was seen in 100% of cells counted, TRM3/4 cytosol signal was seen in 92-100% of cells, and TON1b cytosol signal was seen in 96-100% of cells (3 replicates, n=52, 60, 28, Figure 2.4, Figure 2.1f).

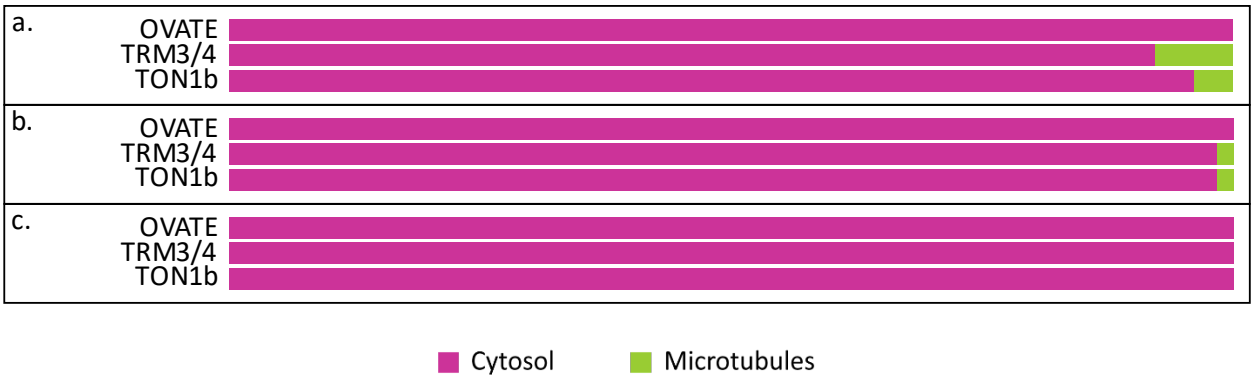

Figure 2.4. Percentage of counted cells with proteins localizing to either the cytosol or microtubules for triple expressions of OVATE + TRM3/4 + TON1b for a) Replicate 1, n=52, b) Replicate 2, n=60, and c) Replicate 3, n=28.

OVATE D280R, TON1b, and TRM3/4 K560V localize in the cytosol when co-expressed

Triple expression for the proteins with mutant interaction domains was examined to test the effect of disassociation between OVATE and TRM3/4 on localization of the whole complex. Triple expression of OVATE D280R, TRM3/4 K560V, and TON1b led to colocalization in the cytosol for all three proteins. OVATE D280R cytosol signal was seen in 100% of cells counted, TRM3/4 K560V cytosol signal was seen in 75-95% of cells, and TON1b cytosol signal was seen in 92-100% of cells (4 replicates, n=26, 20, 12, 12, Figure 2.5, Figure 2.1g).

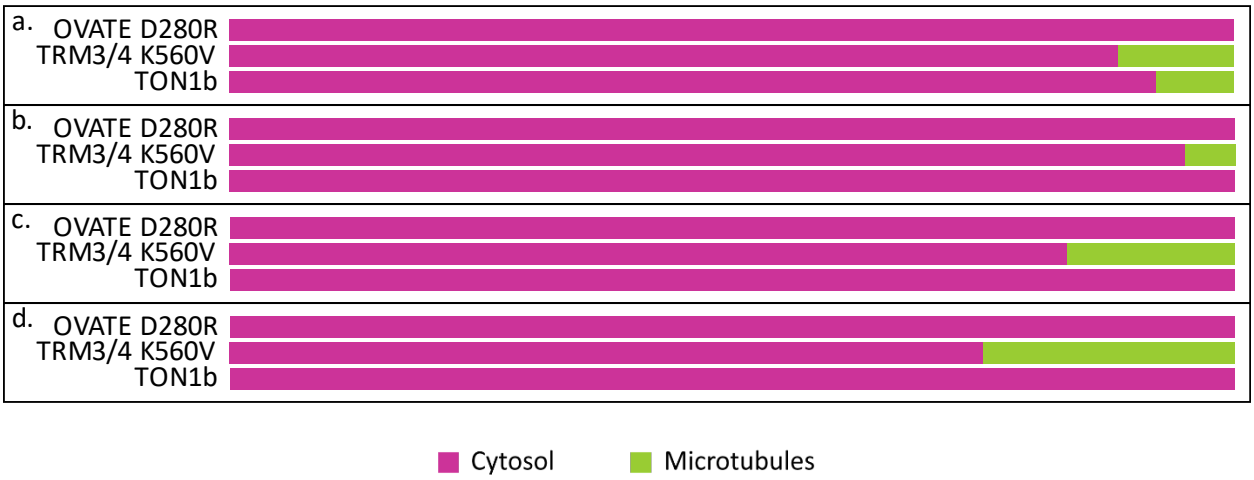

Figure 2.5. Percentage of counted cells with proteins localizing to either the cytosol or microtubules for triple expressions of OVATE D280R + TRM3/4 K560V + TON1b in a) Replicate 1, n=26, b) Replicate 2, n=20, c) Replicate 3, n=12, and d) Replicate 4, n=12.

OVATE and TON1b may interact in the cytosol

Counting cells containing co-expressing OVATE and TON1b was challenging because both are cytosolic proteins when singly expressed. However, when OVATE and TON1b were co-expressed, the OVATE signal displayed characteristics of TON1b localization that were not present in the single expression. There were more cytosolic strands and an outline of the nucleus, and these features overlap for OVATE and TON1b (Figure 2.6a). This trend was also visible in co-expressions of OVATE D280R and TON1b (Figure 2.6b). All cells observed displayed this pattern.

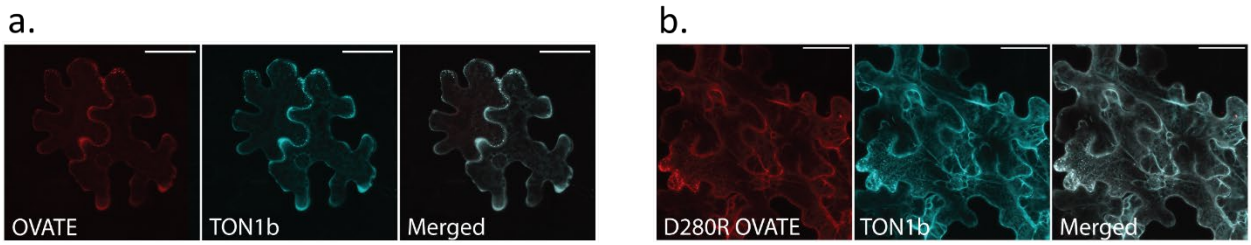

Figure 2.6. Double expression of a) OVATE and TON1b and b) OVATE D280R and TON1b. Bars are 50 μm.

OFP20 localizes to the microtubules when expressed with TRM3/4 and TON1b

When expressed singly, OFP20 localized to the nucleus and cytosol (Figure 2.8a). When co-expressed with TRM3/4, OFP20 and TRM3/4 colocalized to the microtubules while OFP20 also had nuclear signal (Figure 2.7a, Figure 2.8b). This result does not agree with previous studies, which found the majority of TRM3/4 in the cytosol and OFP20 in the cytosol and nucleus. When TRM3/4 and TON1b were co-expressed both localized to the microtubules as before (Figure 2.7b, Figure 2.8c). Preliminary results suggested that when OFP20, TRM3/4, and TON1b are triple expressed, all three proteins colocalized 100% to the microtubules with most OFP20 also showing some nuclear signal (n=43, Figure 2.7c, Figure 2.8d).

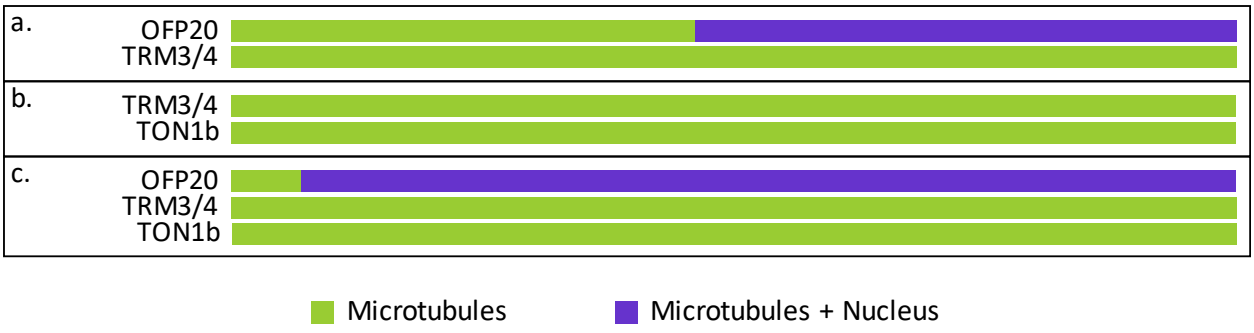

Figure 2.7. Percentage of counted cells with proteins localizing to either the microtubules or microtubules and nucleus for double expressions of a) OFP20 + TRM3/4, n=13, b) TRM3/4 + TON1b, n=15, and c) OFP20 + TRM3/4 + TON1b, n=43.

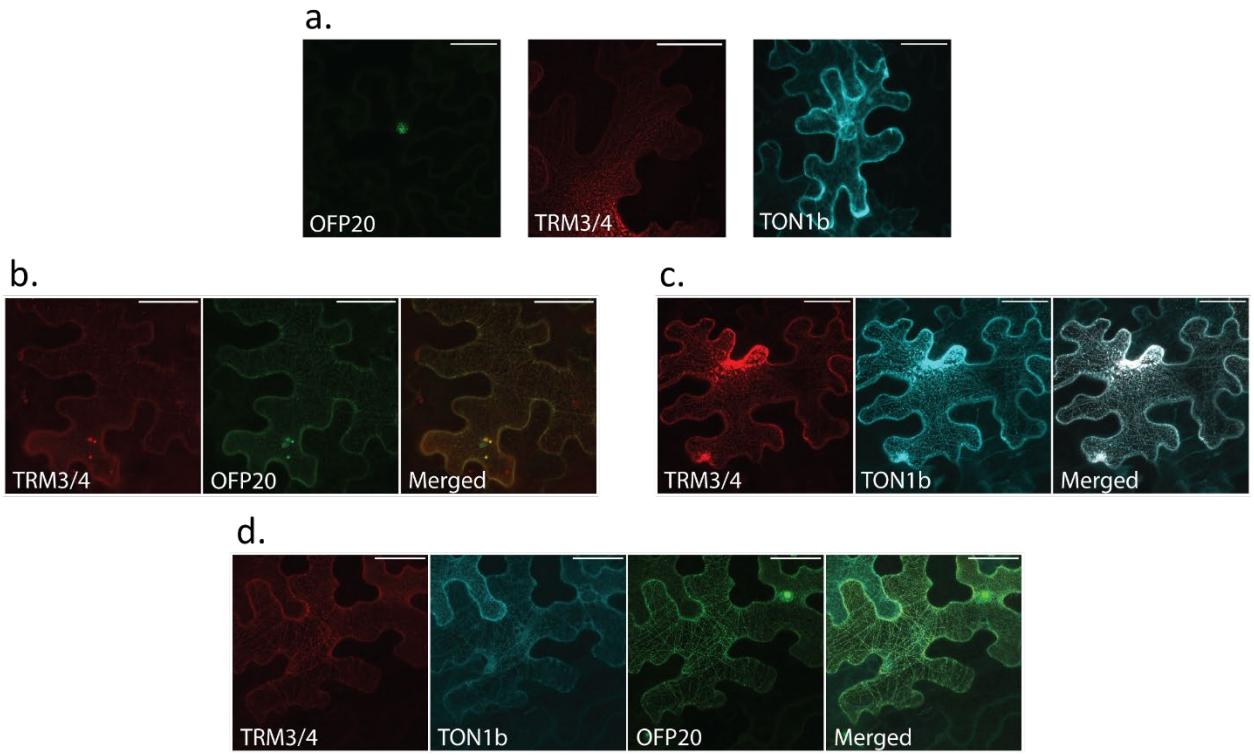

Figure 2.8. Subcellular localization patterns of a) singly expressed proteins, b) double expressed OFP20 + TRM3/4, c) double expressed TRM3/4 + TON1b, d) triple expressed OFP20 + TRM3/4 + TON1b. Bars are 50 μm.

Discussion

This study provides evidence for the hypothesis that OVATE can re-localize the TRM/TON protein complex. Re-localization of this complex could affect cell division because TON1 and the TTP complex are important for organization of the cortical microtubules and formation of the PPB (Spinner et al., 2013). When OVATE was triple expressed with TRM3/4 and TON1b, all three proteins colocalized in the cytosol. TRM3/4 expressed singly and co-expression of TRM3/4 and TON1b both led to localization in the microtubules, so OVATE affected the result of the triple expression. When TRM3/4 and OVATE were co-expressed they colocalized to the cytosol, so it appears that OVATE removed TRM3/4 and TON1b from the microtubules and relocated them to the cytosol.

The expectation was that the interaction between the OFP domain of OVATE and the TRM3/4 M8 motif was the main driver of the protein complex re-localization. To test this hypothesis, the OVATE D280R and TRM3/4 K560V mutants were expressed with TON1b. If OVATE D280R was no longer able to interact with the combination of TRM3/4 K560V and TON1b, then the OVATE D280R signal should have been in the cytosol and the TRM3/4 K560V and the TON1b signals should have been in the microtubules. However, all three proteins colocalized in the cytosol just like the wild type constructs. This result led to the examination of co-expressed OVATE and TON1b. Preliminary observations suggest that both OVATE and OVATE D280R had some interaction with TON1b in the cytosol. This interaction could explain the cytosolic localization of the mutants, because OVATE D280R could recruit TON1b to the cytosol

even if it could not interact with TRM3/4 K560V. TRM3/4 would be pulled to the cytosol by its unaffected interaction with TON1b via its M2 motif.

The interactions of OFP20 with TRM3/4 and TON1b were also examined (Figure 2.8). OFP20 expressed by itself localized to the nucleus and cytosol. When OFP20 was expressed with TRM3/4 both proteins localized in the microtubules, with OFP20 signal still in the nucleus. Triple expressed OFP20, TRM3/4, and TON1b also localized to the microtubules, although TON1b signal was weakest. The interactions of OFP20 with TRM3/4 and TON1b indicate this protein could also be associated with the TTP complex. However, the results of the OFP20 and TRM3/4 double expression do not agree with previous results, so more replicates are needed. Future experiments could also examine triple expression patterns between TON1b and OFP20 and TRM3/4 with mutant interaction domains.

A limitation of this study was a small sample size per replicate for the triple expressed proteins. The initial plan was to count 100 cells per replicate. However, it was challenging to find cells with a good expression level for all three proteins. A low percentage of cells adequately expressed OVATE. Of those, almost all expressed TON1b but fewer also expressed TRM3/4. Additionally, the RFP-TRM3/4 construct had poor expression and OFP20 had low cytosol signal. These low expressions may have affected the proper scoring of protein localization.

Further research should examine the colocalization of OVATE and TON1b with other TRMs, especially TRM5. TRM5 was not examined in this study because the expression of that construct is challenging and was not possible in the time limit of this

study. Further research with OFP20 would also be beneficial, especially since the double mutants of OVATE and OFP20 have such a striking effect on fruit shape.

CHAPTER 3

OVATE, SOV1, AND TRM5 REGULATE ORGAN SHAPE DURING FLOWER BUD DEVELOPMENT[1]

[1]Kraus, C.O. and E. van der Knaap. To be submitted to *Plant Biology*.

Abstract

Wild tomatoes are small and round, but cultivated tomatoes have many shapes and sizes. A few tomato fruit shape genes, *SUN*, *OVATE*, *SlOFP20* (*SOV1*), *LC*, and *FAS*, have been cloned. *OVATE* is highly expressed in young floral organ primordia during early flower development. Wild tomato NILs with *ovate/sov1* mutations produce pear-shaped fruit due to histological changes at the proximal end and their flowers at anthesis display an ovary shape similar to that of the final fruit. OVATE interacts with microtubule associated TRM5 both genetically and biochemically. TRM5 has a similar expression pattern to OVATE and the *trm5* mutation restores the round fruit phenotype in tomato NILs when introduced into the pear-shaped *ovate/sov1* background. This study investigated the developmental timing of these genes on ovary shape. We optimized a protocol to clear the tissues, stain the cell walls with a fluorescent dye, and take images using a confocal microscope. Early flower bud developmental stages were examined with three experiments using 10-15 inflorescences each of the NILs for *ovate/sov1* and *ovate/sov1/trm5*, and wild type accession LA1589. Buds four, six, seven, and nine days post floral initiation were used. Medial-lateral length and cell count measurements were taken of the developing carpel primordia and whole bud shape index. The data indicate that buds with *ovate/sov1* mutations have a narrower medial-lateral length and smaller medial-lateral cell count than WT LA1589 at seven days post-initiation. These results suggest that OVATE affects ovary patterning early in gynoecium development. At this early stage the *ovate/sov1/trm5* triple mutants already displayed a similar phenotype to LA1589.

Introduction

Tomato is a good model species to study fleshy fruit growth and development because it has a basic fruit structure and a relatively short generation time. Tomato is botanically a berry and arises from a simple, perfect flower. The tomato inflorescence is a cyme, and it grows through the inflorescence meristem splitting into a terminating floral meristem and a new inflorescence meristem (Welty et al., 2007). Wild tomato accession LA1589 (*Solanum pimpinellifolium*) produces on average one flower per day and around 20 flowers per inflorescence, and the flowers take 19 days to mature (Xiao et al., 2009). Wild tomato plants produce small, round fruits. Before domestication, the pressure of fruit-eating animals like birds selected for easily eaten fruits (Lord, 2004). Small size and round shape are beneficial for the wild plant because these animals easily consume the fruits and disperse the seeds.

Cultivated tomatoes have a variety of shapes and sizes. Several tomato fruit shape genes, namely *SUN*, *OVATE*, *SlOFP20* (*SOV1*), *LC*, and *FAS*, have been cloned (Rodríguez et al., 2011; Wu et al., 2018). The mutations in these genes arose during domestication (Blanca et al., 2015; Wu et al., 2018). Cultivated tomato (*Solanum lycopersicum* var. *lycopersicum*) accessions with a mutation of *ovate* are often oblong or obovate in shape, but some accessions are round (Rodríguez et al., 2013). This difference in fruit shapes between cultivars carrying the *ovate* mutation led to the cloning of Suppressor Of OVATE (SOV1), which was later determined to be OFP20 (Wu et al., 2018). *OVATE* and *SOV1* both appear in semi-cultivated tomato accessions (*Solanum lycopersicum* var. *cerasiforme*), but not in the same accession. Most cultivars that have both *ovate* and *sov1* mutations have pear-shaped fruit (Wu et al., 2018).

Members of the OVATE Family Proteins (OFPs) also regulate organ shape in other plant species, including *Arabidopsis*, rice, potato, and melon (Schmitz et al., 2015; Wang et al., 2007; Wang et al., 2011; Wu et al., 2018).

Nearly isogenic lines (NILs) with *ovate/sov1* mutations in the wild type LA1589 background produce pear-shaped fruit. *OVATE* is highly expressed in young floral primordia as they arise in the developing flower bud (Wu et al., 2018). This interesting pear shape is due to histological changes at the proximal end of the fruit caused by more cells in the proximal-distal axis and less cells in the medial-lateral axis. The ovaries of the flowers at anthesis already display a shape similar to that of the final fruit (van der Knaap et al., 2014; Wu et al., 2018).

A Yeast 2-Hybrid (Y2H) screen with OVATE as the bait pulled down 11 of the 26 known TONNEAU1 Recruiting Motif (TRM) proteins in tomato, including several microtubule-associated TRMs (van der Knaap et al., 2014). *TRM5* is an especially interesting member of this family because this gene has a similar expression pattern with *OVATE* and TRM5 falls within the AtTRM1-5 subclade (Wu et al., 2018). *AtTRM1* and *AtTRM2* affect organ shape of leaves, flowers, and fruits in *Arabidopsis* by regulating cell elongation (Lee et al., 2006). When introduced into the pear-shaped *ovate/sov1* background, the *trm5* mutation restores the round fruit phenotype in NILs, which is also visible at anthesis (Wu et al., 2018). OVATE interacts with TRM5 and when co-expressed in *Nicotiana benthamiana*, it relocalizes TRM5 from the microtubules to the cytoplasm (Wu et al., 2018). Members of the TRM family interact with TONNEAU1 (TON1) to target the TRM/TON/PP2A (TTP) complex to the microtubules (Drevensek et al., 2012; Spinner et al., 2013). The TTP complex

associates with the cortical microtubules and the pre-prophase band (PPB) during cell division, indicating its potential importance in organizing the microtubules (Spinner et al., 2013).

This study examines how early in the development of the flower these genes affect ovary shape. Previous studies indicate that these genes affect fruits and flowers, but no studies have examined earlier stages prior to flower opening. We expected to find shape differences between the accessions after the carpel had emerged from the remaining meristem, but before anthesis.

Methods

Plant materials and collection

The existing NILs for *ovate/sov1* and *ovate/sov1/trm5* as well as wild type *S. pimpinellifolium* accession LA1589 were used. There are two different frameshift *trm5* mutants, one resulting from a 1bp insertion and the other from a 1bp deletion, but both display the same phenotype.

Three replicates of this experiment were conducted. Experiment 1 used 72 seedlings each of wild type LA1589, *ovate/sov1*, and *ovate/sov1/trm5* which were sown in seedling flats on May 18, 2018 and kept in the growth chamber at 30°C until the plants emerged. The flats were transferred to the greenhouse until the plants initiated flowering. When at least 6 buds were visible to the naked eye, the entire inflorescence was removed with forceps. At this stage the inflorescence meristem was still dividing and there were at least 10 buds (about 6 easily visible) of which the last should correspond to floral stage 8 (10 days post floral initiation) (Welty et al., 2007). Buds

were collected on June 22 and 24, 2018. The floral development stages of 4, 6, 7, and 9 days post initiation (dpi) were compared across the different accessions.

Experiment 2 used inflorescences from older plants sown by Biyao Zhang in October 2018. Four replicate plants each of LA1589, *ovate/sov1*, and *ovate/sov1/trm5* were used. Six inflorescences were collected from side shoots of each of these plants and removed when at least five buds were visible to the unaided eye.

For Experiment 3, one tray each of LA1589, *ovate/sov1*, and *ovate/sov1/trm5* were sown on December 26, 2018 and kept in the growth chamber at 30°C. Each tray contained 32 pots and seedlings were weeded so only two seedlings per pot remained, yielding 64 total seedlings for each accession. Once all the seedlings had emerged, the trays were transferred to the greenhouse. The third and fourth inflorescences with at least five buds visible (and no open flowers) were collected on March 1, 2019.

Bud clearing protocol

The following methods to clear and stain early-stage tomato buds for visualization on a confocal microscope are based on a protocol from Schaefer et al. (2017). The buds were placed in 15 ml falcon tubes for fixation overnight with a solution of 75% ethanol and 25% acetic anhydride. The next day the buds were heated in the water bath for 10 minutes in 80% ethanol at 80°C for permeabilization. Afterward, the buds were rehydrated for 10 minutes in 50% ethanol at room temperature, for another 10 minutes in 30% ethanol, and then for 10 minutes in water. To clear the buds, they were gently agitated on a rocker in a solution of 0.2N NaOH and 1% SDS for 24 hours and then in a solution of ClearSee (10% xylitol, 15% deoxycholic acid sodium salt, 25% urea) for 3 days. Afterward, the buds were washed for 5 minutes in water and then

stained in Calcofluor (Fluorescent Brightener 28 and a few drops of 10N NaOH) for 30 minutes at room temperature. Using a dissecting microscope, the inflorescences were mounted on a slide with Citifluor. The buds can be stored in this media for several weeks at room temperature. Two small pieces of double-sided tape were used to raise the coverslip over the bud. The slides were stored for future use.

Image acquisition and processing

The buds were excited at 405 nm and viewed using a confocal microscope. The pinhole was set at 29.9 μm. The gain was adjusted in the range of 300-600 V to optimize the exposure of the image to facilitate cell counting. The resolution was set to 1024x1024 pixels. Z-stack images were taken of the whole carpel to facilitate finding the center of the organ.

ImageJ was used to measure the flower buds. The medial/lateral width of the remaining meristem was measured for the 4 dpi flower buds, and the medial/lateral width of the developing carpel was measured for the 6, 7, and 9 dpi buds. The medial/lateral width was measured at the base of the carpel, between the inflection points where the emerging sepals/petals meet the developing carpel. The number of cells were counted along this medial/lateral distance. The medial/lateral width and the proximal/distal height of the whole bud were also measured to determine the whole bud shape index, which is calculated by the ratio of maximum proximal/distal height to medial/lateral width (Brewer et al., 2006). Between 10-25 buds per accession were measured. Cell medial/lateral width and proximal/distal length were measured for 5-7 buds from Experiment 3. The mean values of these different measurements were

compared between the different accessions using a Student's t-test in JMP to quantify the differences in shape between the NILs.

Expression data

The RNA-Seq normalized expression data were downloaded from files available on the Tomato Functional Genomics Database (D015 and D016, http://ted.bti.cornell.edu/cgi-bin/TFGD/digital/home.cgi). These data were collected from *S. pimpinellifolium*. Four replicates each of the inflorescence/floral meristem and 2, 4, and 6 day old flower bud tissues were collected, with over 100 buds per replicate (D015; Chu et al., in press). Two replicates of the anthesis flowers were collected, with 10 replicates (D016; Wu et al., 2018).

Results

OVATE, TRM5, and SOV1 are expressed in floral development

Many genes are active during the organization and differentiation of tissues in the developing meristem and flower bud. Mutations of *ovate/sov1* result in an elongated ovary and ultimately a striking final fruit phenotype suggesting these genes have a role during floral development (Table 3.1). At anthesis, the elongation of the *ovate/sov1* NIL and the restoration of wild type phenotype in the *ovate/sov1/trm5* NIL is already visible (Wu et al., 2018). Therefore, we investigated when during floral development these genes are expressed and act to regulate ovary shape.

OVATE, *SOV1*, and *TRM5* are all expressed in young flower buds of wild type LA1589. *OVATE* and *TRM5* shared a similar expression pattern and were most highly

expressed in early flower buds (Figure 3.1). SOV1 had low expression during the young flower bud stages but is highly expressed at anthesis (Wu et al., 2018).

Table 3.1. Fruit phenotypes of the different NILs used in the experiment.

			
Name	LA1589	SA38	SA37
Mutation	Wild type	*ovate/sov1*	*ovate/sov1/trm5*
Phenotype	Round ovary and fruit	Elongated ovary and fruit	Round ovary and fruit

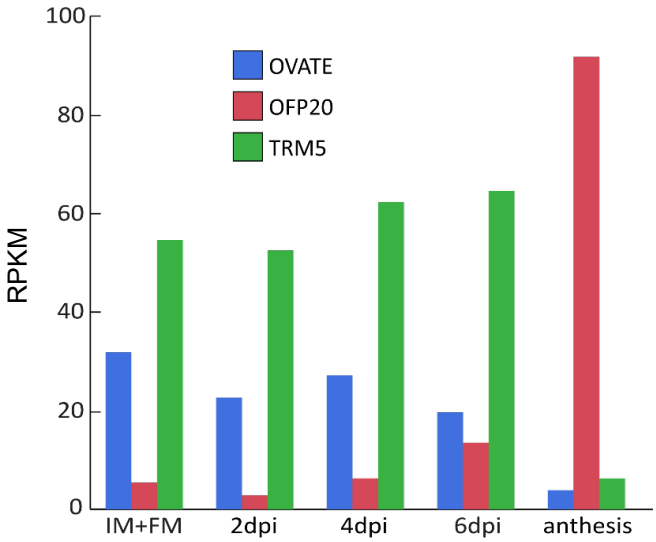

Figure 3.1. Expression levels of *TRM5*, *OVATE*, and *SOV1* at different floral development stages. RPKM, reads per kilobase of transcript per million reads.

OVATE, SOV1, and TRM5 affect developing ovary width as early as 7 dpi

Flower growth in *S. pimpinellifolium* progresses through several key developmental landmarks that are defined by the emergence and growth of different

structures (Xiao et al., 2009). At 4 dpi, the sepals have emerged and elongated to cover the remaining meristem and the petal primordia are beginning to arise (Figure 3.2a). At 6 dpi, the carpel primordium is beginning to arise (Figure 3.2b). The carpel primordium continues to elongate at 7 dpi (Figure 3.2c). By 9 dpi the style elongates and the ovule primordia are emerging (Figure 3.2d; Xiao et al., 2009).

Ovary medial/lateral distance were measured over three experiments in buds 4, 6, 7, and 9 days post initiation (dpi) (Figure 3.2). The *ovate/sov1* double mutants and *ovate/sov1/trm5* triple mutants were compared with wild type LA1589. In all three experiments, medial/lateral distance of ovaries at 4 dpi were not different between the three accessions (Figure 3.3). At 6 dpi, the ovary medial/lateral distance was not significantly different in Experiment 1. However, in Experiments 2 and 3, the ovaries at 6dpi of *ovate/sov1/trm5* and wild type had significantly larger medial/lateral ovary lengths than *ovate/sov1*. At 7 dpi in all three experiments the *ovate/sov1* ovaries had significantly smaller medial/lateral ovary lengths than wild type, and were significantly smaller than *ovate/sov1/trm5* in Experiments 2 and 3. At 9 dpi, the trend of smaller medial/lateral ovary length for the *ovate/sov1* double mutants was continued in Experiments 1 and 3. In Experiment 2 at 9 dpi, the double and triple mutant ovary medial/lateral length were not significantly different from wild type.

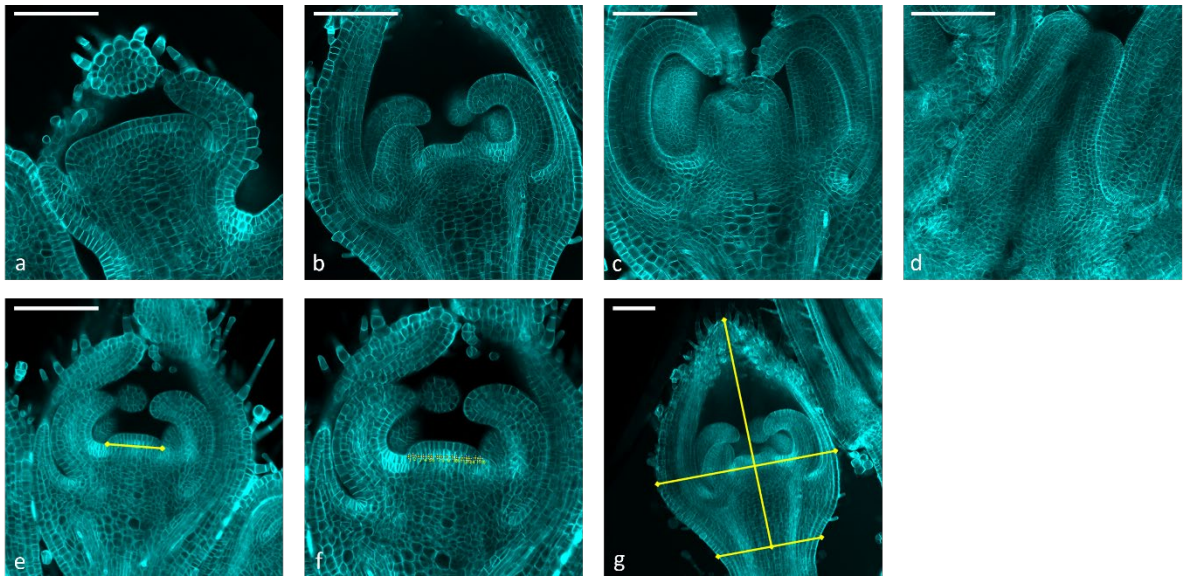

Figure 3.2. Buds from a single LA1589 accession in Experiment 2. Bud stages are shown at a) 4 dpi, b) 6 dpi, c) 7 dpi, and d) 9 dpi. Measurements were made of the e) medial/lateral ovary width, f) medial/lateral cell count, and g) whole bud shape index. The buds pictured in e-g are 6 dpi. The scale bar is 100 µm.

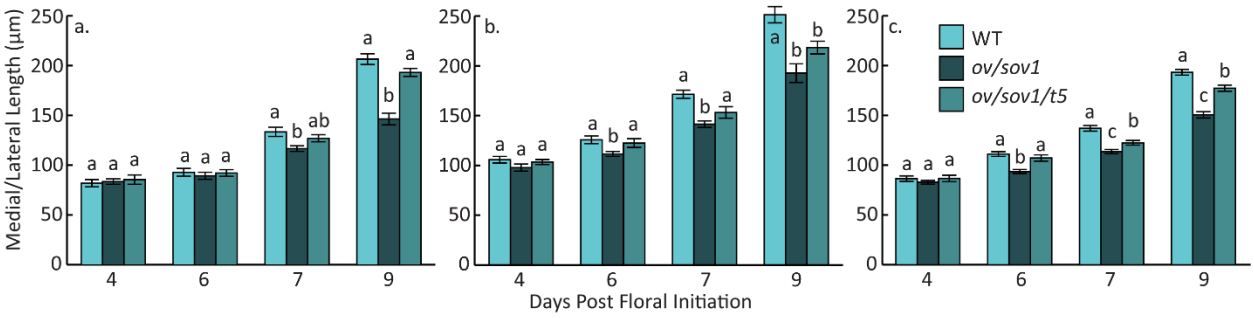

Figure 3.3. Medial-lateral length measurements of young tomato flower buds. The remaining meristem and early carpel primordia were measured for buds 4 days post initiation (dpi), 6 dpi, 7 dpi, and 9 dpi. This experiment was repeated three times, with a) the first inflorescence of young seedlings, b) inflorescences of mature plants, and c) older inflorescences of seedlings. Bars represent standard error.

OVATE, SOV1, and TRM5 affect cell number in the developing ovary as early as 7 dpi

The number of cells along the measured medial/lateral distance were counted for each accession (Figure 3.2). In Experiments 1 and 3, the number of cells was not significant between the accessions at 4 dpi (Figure 3.4). In Experiment 2 at 4 dpi, *ovate/sov1* and *ovate/sov1/trm5* were significantly different from each other while neither was significantly different form LA1589. At 6 dpi, the experiments were not significantly different in Experiment 1. However, at 6 dpi in Experiment 2 *ovate/sov1* had significantly fewer cells than *ovate/sov1/trm5* and in Experiment 3 wild type had significantly more cells than both *ovate/sov1* and *ovate/sov1/trm5*. In all three experiments at 7 dpi wild type had significantly more cells than *ovate/sov1*. At 9 dpi in all three experiments wild type also had significantly more cells than *ovate/sov1.* In Experiment 2 at 9dpi there was no significant difference between the accessions, while in Experiment 3 all three accessions were significantly different from each other, with *ovate/sov1* having the lowest cell count.

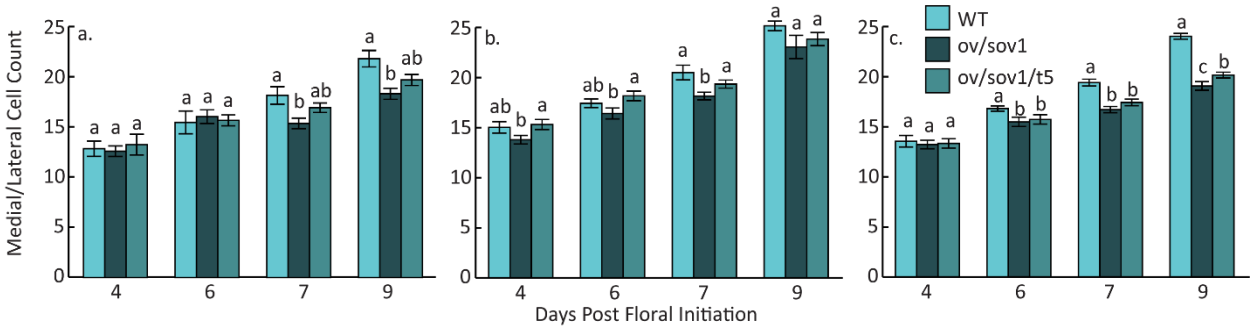

Figure 3.4. Cell counts along the medial-lateral axis for young tomato flower buds. Cells in the remaining meristem and early carpel primordia were counted in buds 4 days post initiation (dpi), 6 dpi, 7 dpi, and 9 dpi. This experiment was repeated three times, with a) the first inflorescence of young seedlings, b) inflorescences of mature plants, and c) older inflorescences of seedlings. Bars represent standard error.

OVATE, SOV1, and TRM5 affect bud shape index as early as 4 dpi

Shape index (measured as maximum height divided by maximum width) is a useful measure of fruit shape (Brewer et al., 2006). This process was extended to flower buds to compare their overall shapes. Shape index was measured for 4 and 6 dpi flower buds in Experiment 1 and for 4, 6, and 7 dpi buds in Experiments 2 and 3. In Experiment 1, the shape index of *ovate/sov1* was significantly larger than *ovate/sov1/trm5* at 4dpi but neither were significantly different from LA1589 (Figure 3.5). In Experiment 2, *ovate/sov1/trm5* and LA1589 were significantly different from *ovate/sov1* at 4 dpi. At 6 dpi in all three experiments the *ovate/sov1* double NIL had a significantly larger shape index than the wild type and *ovate/sov1/trm5* accessions. In addition, in Experiment 2 at 6 dpi the *ovate/sov1/trm5* triple NIL had a significantly smaller shape index than the wild type. Experiments 2 and 3 had the same pattern at 7

dpi, with the *ovate/sov1* shape index significantly larger than wild type, and the wild type shape index significantly larger than *ovate/sov1/trm5* (Figure 3.5). This difference in shape index was predominately driven by a narrower medial/lateral width in the *ovate/sov1* accessions and a shorter proximal/distal length in the *ovate/sov1/trm5* accessions at 6 and 7 dpi (Figures 3.6 and 3.7).

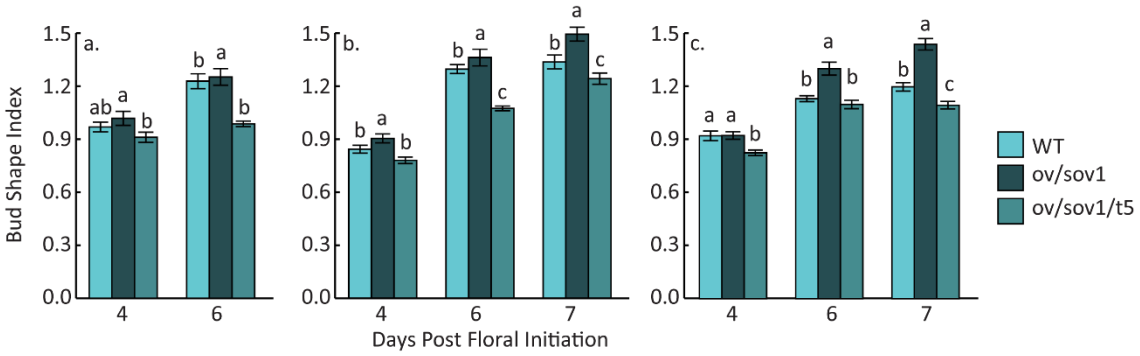

Figure 3.5. The shape index of the whole bud was measured as the ratio of maximum height to maximum width. These measurements were collected from buds 4 days post initiation (dpi), 6 dpi, and 7 dpi. This experiment was repeated three times, with a) the first inflorescence of young seedlings, b) inflorescences of mature plants, and c) older inflorescences of seedlings. Bars represent standard error.

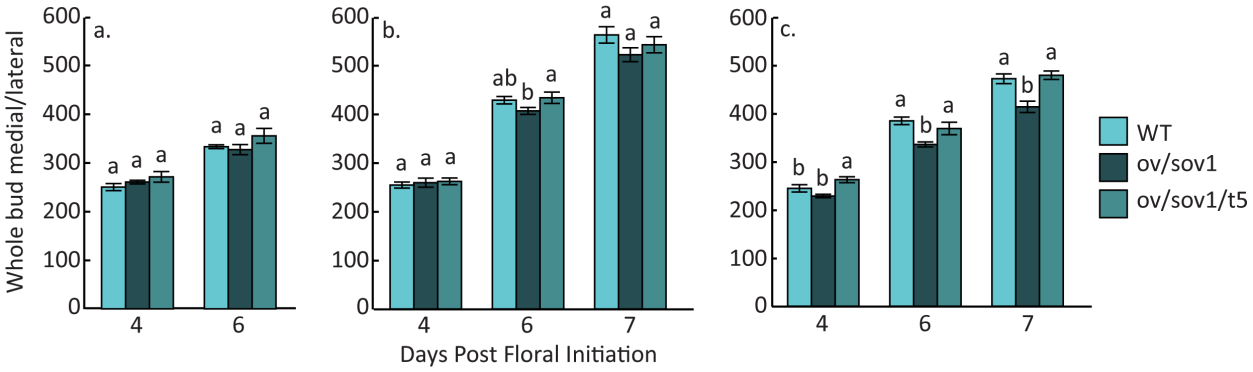

Figure 3.6. Medial/lateral width for whole buds. These measurements were repeated three times in a) Experiment 1, b) Experiment 2, and c) Experiment 3. Bars represent standard error.

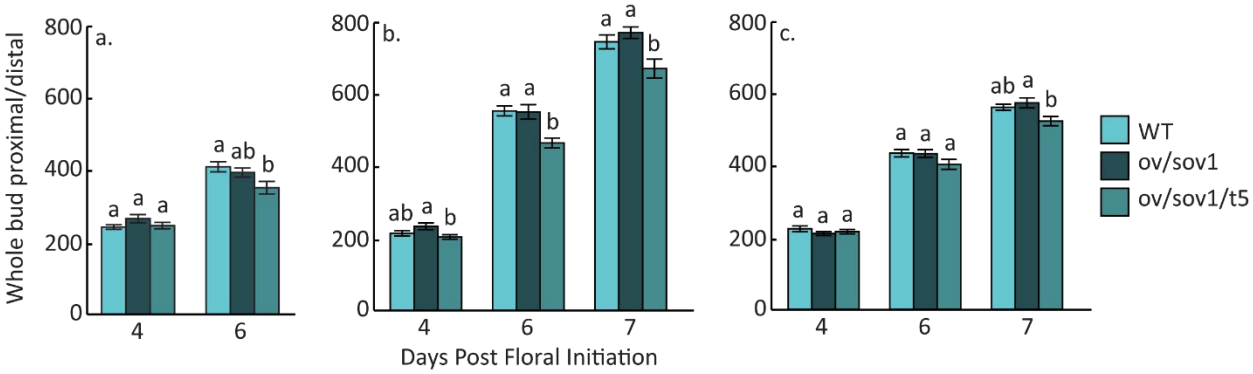

Figure 3.7. Proximal/distal length for whole buds. These measurements were repeated three times in a) Experiment 1, b) Experiment 2, and c) Experiment 3. Bars represent standard error.

Preliminary cell shape measurement in developing ovaries

The medial/lateral width of the developing ovaries and cell count along this axis were known so the width was divided by the cell count to provide an approximate medial/lateral cell width (Figure 3.8). In all three experiments the cells at 4, 6, and 7 dpi

show no significant difference in medial-lateral cell width. In 9 dpi buds the cells of *ovate/sov1* ovaries are significantly narrower than WT and *ovate/sov1/trm5* in Experiments 1 and 2, and significantly narrower than *ovate/sov1/trm5* in Experiment 3.

Cell dimensions were measured by hand of a subset of buds (n=5-7) from Experiment 3 (Figure 3.9). A similar trend of cell medial/lateral width is observed between Figures 3.8c and 3.9a, which correspond to the same experiment, although the WT cells are narrower in the hand-measured cells. Cell proximal/distal length was not significantly different between the three accessions at any of the days measured. The *ovate/sov1/trm5* cell shape index (maximum length divided by maximum width) was significantly smaller than WT at 4 and 9 dpi, while *ovate/sov1* was not significantly different from either (Figure 3.9c).

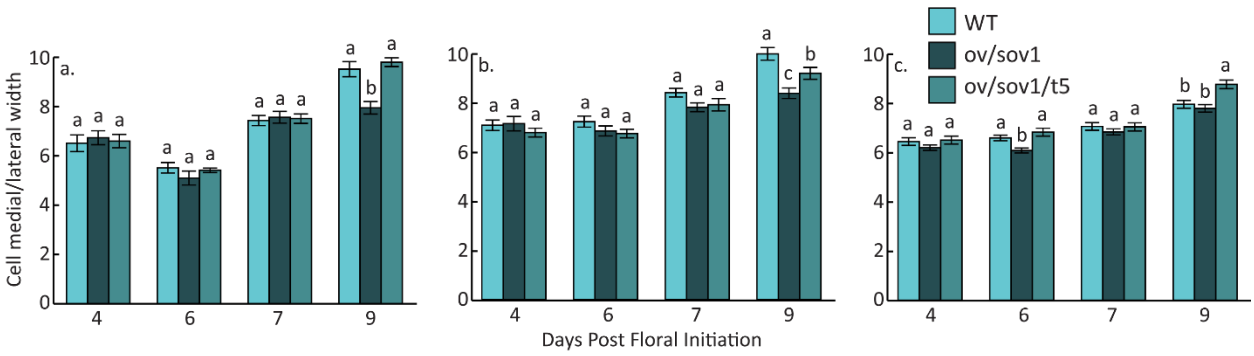

Figure 3.8. Medial/lateral width of cells determined by dividing the medial/lateral ovary length by the cell number for a) Experiment 1, b) Experiment 2, and c) Experiment 3. Bars represent standard error.

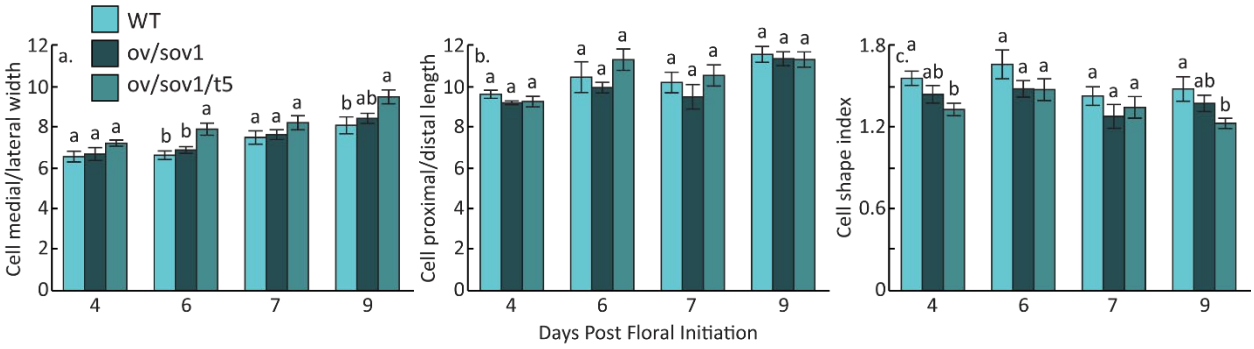

Figure 3.9. Ovary cell measurements of buds from Experiment 3. Measurements of a) cell medial/lateral width, b) cell proximal/distal length, and c) shape index were taken. Shape index is maximum length divided by maximum width. Bars represent standard error.

Discussion

This study examined developing flower bud and ovary shape to determine when during floral development the effect of the fruit shape genes *OVATE*, *SOV1*, and *TRM5* is visible. Ovary shape differences between wild type, *ovate/sov1,* and *ovate/sov1/trm5* accessions are clearly visible in the final fruit and in the ovaries at anthesis, but the timing of their expression suggests these genes function much earlier in bud development (Table 3.1; Figure 3.1; Wu et al., 2018). Wild tomato *S. pimpinellifolium* flowers take 19 days to mature, but the morphological changes that lead to different fruit shape occur long before the flower opens (Xiao et al., 2009).

The effects of the fruit shape genes *OVATE*, *SOV1*, and *TRM5* on the developing ovary were visible between 6 and 7 dpi. The 4 dpi flower buds of wild type, *ovate/sov1*, and *ovate/sov1/trm5* did not vary significantly across genotype for medial lateral length and cell count (Figures 3.3 and 3.4). However, at 7 dpi, buds with *ovate/sov1* mutations

had a narrower medial-lateral length and smaller medial-lateral cell count than wild type. At this early stage the *ovate/sov1/trm5* triple mutants already display a similar phenotype to wild type. There was some variability within and between the experiments. The floral primordia grow very rapidly so not all the buds selected are at an identical growth stage. Care was taken to choose buds at as similar a stage as possible, but there is some variation. It was especially difficult to find 6 dpi buds of the correct size because the carpel elongates so quickly at this stage. The experiments came from plants of three different ages, and were collected at different times of the year, explaining some of the variability between the experiments. The inflorescences from Experiment 3 came from older seedling inflorescences because the first inflorescence of ovate/sov1 showed damage (Appendix A, potential cell wall instability).

These results suggest that OVATE affects ovary patterning early in gynoecium development, when the carpel is arising and extending, and that TRM5 functions at a similar time. Buds with *ovate/sov1* mutations have a larger shape index than wild type or *ovate/sov1/trm5* as early as 4 dpi (Figure 3.5). Specifically, the *ovate/sov1* buds have a narrower medial/lateral width than WT and *ovate/sov1/trm5* and the *ovate/sov1/trm5* buds have a shorter proximal/distal length than WT and *ovate/sov1*. These results indicate that OVATE and TRM5 affect other flower organs than the carpel, and that the *trm5* mutation can restore this phenotype to wild type accessions. TRM5 affects many plant organs including leaf shape (Wu et al., 2018). TRM5 is already active in the tomato meristem and early flower buds (Figure 3.1). Sepal primordia have already emerged and elongated at 4 dpi, so TRM5 could already have acted to affect sepal size.

This study indicates that the effects of OVATE, SOV1, and TRM5 function to affect bud shape as early as 6 or 7 dpi, where there was a significant difference in carpel shape (Figure 3.3). However, these data do not reveal which gene is functioning first. The *ovate/sov1* mutation leads to an extreme phenotype which was useful in determining when these genes function in bud development. This finding begs the question of whether the genes all function synchronously or in a different order. Future research could examine more closely early stage flower buds of single mutants of *ovate* and *sov1*, which show much subtler phenotypes than the double mutant, or of other fruit shape genes (Appendix B, interactions of *sun* with *ovate*, *sov1*, and *trm5* in mature fruit). Future experiments should also investigate cell shape during ovary development, as there is preliminary evidence of differences in medial/lateral cell width (Figures 3.8 and 3.9).

CHAPTER 4

CONCLUSION

Humans have long been fascinated by fruit shape, and varied fruit shapes satisfy different market classes and consumer preferences. Investigating OFPs, TRMs, and TON1 could lead to a better understanding of the mechanisms that affect fruit shape. Through protein localization studies we found that OVATE can re-localize the TRM3/4-TON1 protein complex to the cytosol, but the interaction is more complex. OVATE may interact with TON1 and future research should explore this possibility. OVATE, SOV1, and TRM5 are all expressed early in gynoecium development. We see an effect of these genes on ovary and bud shape at the early stage of 6-7 days post floral initiation. The *OVATE* and *TRM5* genes appear to function at a similar time, and the *ovate/sov1/trm5* triple mutant already restores wild type phenotype in these young carpels. Future research should focus on these stages and further investigate other genotypes and TRMs. OVATE Family Proteins are found in all land plants and are important in other crop species such as potato and melon. This research helps inform how fruit shape develops and provides a framework of how shape variation is determined in other crops.

REFERENCES

Azimzadeh, J., P. Nacry, A. Christodoulidou, S. Drevensek, C. Camilleri, N. Amiour, et al. 2008. Arabidopsis TONNEAU1 proteins are essential for preprophase band formation and interact with centrin. The Plant Cell: 2146. doi:10.1105/tpc.107.056812.

Blanca, J., J. Montero-Pau, C. Sauvage, G. Bauchet, E. Illa, M.J. Díez, et al. 2015. Genomic variation in tomato, from wild ancestors to contemporary breeding accessions. BMC Genomics 16: 257-257. doi:10.1186/s12864-015-1444-1.

Brewer, M.T., L. Lang, K. Fujimura, N. Dujmovic, S. Gray and E. van der Knaap. 2006. Development of a controlled vocabulary and software application to analyze fruit shape variation in tomato and other plant species. Plant Physiol 141: 15-25. doi:10.1104/pp.106.077867.

Camilleri, C., J. Azimzadeh, M. Pastuglia, C. Bellini, O. Grandjean and D. Bouchez. 2002. The Arabidopsis TONNEAU2 gene encodes a putative novel protein phosphatase 2A regulatory subunit essential for the control of the cortical cytoskeleton. The Plant Cell: 833.

Chu, Y.H., J.-C. Jang, Z. Huang and E. van der Knaap. in press. Tomato locule number and fruit size controlled by natural alleles of lc and fas. Plant Direct.

Drevensek, S., M. Goussot, Y. Duroc, A. Christodoulidou, S. Steyaert, E. Schaefer, et al. 2012. The Arabidopsis TRM1-TON1 interaction reveals a recruitment network common to plant cortical microtubule arrays and eukaryotic centrosomes. The Plant Cell 24: 178-191.

Hackbusch, J., K. Richter, J. Müller, F. Salamini and J.F. Uhrig. 2005. A central role of Arabidopsis thaliana ovate family proteins in networking and subcellular localization of 3-aa loop extension homeodomain proteins. Proceedings of the National Academy of Sciences of the United States of America 102: 4908-4912. doi:10.1073/pnas.0501181102.

Hashimoto, T. 2015. Microtubules in Plants. The Arabidopsis Book 13: e0179. doi:10.1199/tab.0179.

Huang, Z., J. Van Houten, G. Gonzalez, H. Xiao and E. van der Knaap. 2013. Genome-wide identification, phylogeny and expression analysis of SUN, OFP and YABBY gene family in tomato. Molecular Genetics And Genomics: MGG 288: 111-129. doi:10.1007/s00438-013-0733-0.

Ku, H.-M., J. Liu, S. Doganlar and S.D. Tanksley. 2001. Exploitation of Arabidopsis-tomato synteny to construct a high-resolution map of the ovate-containing region in tomato chromosome 2. Genome 44: 470.

Ku, H.-M., S.D. Tanksley, K.Y. Chen and S. Doganlar. 1999. The genetic basis of pear-shaped tomato fruit. Theoretical and applied genetics 99: 844-850.

Lazzaro, M.D., S. Wu, A. Snouffer, Y. Wang and E. van der Knaap. 2018. Plant organ shapes are regulated by protein interactions and associations with microtubules. Frontiers in plant science 9: 1766-1766. doi:10.3389/fpls.2018.01766.

Lee, Y.K., G.-T. Kim, I.-J. Kim, J. Park, S.-S. Kwak, G. Choi, et al. 2006. LONGIFOLIA1 and LONGIFOLIA2, two homologous genes, regulate longitudinal cell elongation in Arabidopsis. Development 133: 4305-4314. doi:10.1242/dev.02604.

Li, E., S. Wang, Y. Liu, J.-G. Chen and C.J. Douglas. 2011. OVATE FAMILY PROTEIN4 (OFP4) interaction with KNAT7 regulates secondary cell wall formation in Arabidopsis thaliana. Plant Journal 67: 328-341. doi:10.1111/j.1365-313X.2011.04595.x.

Liu, D., W. Sun, Y. Yuan, N. Zhang, A. Hayward, Y. Liu, et al. 2014. Phylogenetic analyses provide the first insights into the evolution of OVATE family proteins in land plants. Annals of Botany 113: 1219-1233.

Liu, J., J. van Eck, B. Cong and S.D. Tanksley. 2002. A new class of regulatory genes underlying the cause of pear-shaped tomato fruit. Proceedings of the National Academy of Sciences of the United States of America 99: 13302-13306.

Liu, J., J. Zhang, W. Hu, H. Miao, J. Zhang, C. Jia, et al. 2015. Banana Ovate family protein MaOFP1 and MADS-box protein MuMADS1 antagonistically regulated banana fruit ripening. Plos One 10: e0123870-e0123870. doi:10.1371/journal.pone.0123870.

Liu, Y. and C.J. Douglas. 2015. A role for OVATE FAMILY PROTEIN1 (OFP1) and OFP4 in a BLH6-KNAT7 multi-protein complex regulating secondary cell wall formation in Arabidopsis thaliana. Plant Signaling & Behavior 10.

Lord, J.M. 2004. Frugivore gape size and the evolution of fruit size and shape in southern hemisphere floras. Austral Ecology 29: 430-436. doi:10.1111/j.1442-9993.2004.01382.x.

Pagnussat, G.C., H.-J. Yu and V. Sundaresan. 2007. Cell-fate switch of synergid to egg cell in Arabidopsis Eostre mutant embryo sacs arises from misexpression of the BEL1-like homeodomain gene BLH1. The Plant Cell: 3578. doi:10.1105/tpc.107.054890.

Price, H.L. and A.W. Drinkard. 1909. Inheritance in tomato hybrids. The Plant World: 10.

Rodríguez, G.R., H.J. Kim and E. van der Knaap. 2013. Mapping of two suppressors of OVATE (sov) loci in tomato. Heredity 111: 256-264. doi:10.1038/hdy.2013.45.

Rodríguez, G.R., S. Muños, C. Anderson, S.-C. Sim, A. Michel, M. Causse, et al. 2011. Distribution of SUN, OVATE, LC, and FAS in the tomato germplasm and the relationship to fruit shape diversity. Plant Physiology 156: 275-285. doi:10.1104/pp.110.167577.

Schaefer, E., K. Belcram, M. Uyttewaal, Y. Duroc, M. Goussot, D. Legland, et al. 2017. The preprophase band of microtubules controls the robustness of division orientation in plants. Science 356: 186. doi:10.1126/science.aal3016.

Schmitz, A.J., K. Begcy, G. Sarath and H. Walia. 2015. Rice Ovate Family Protein 2 (OFP2) alters hormonal homeostasis and vasculature development. Plant Science: An International Journal Of Experimental Plant Biology 241: 177-188. doi:10.1016/j.plantsci.2015.10.011.

Spinner, L., A. Gadeyne, K. Belcram, M. Goussot, M. Moison, Y. Duroc, et al. 2013. A protein phosphatase 2A complex spatially controls plant cell division. Nature Communications 4: 1863. doi:10.1038/ncomms2831.

Spinner, L., M. Pastuglia, K. Belcram, M. Pegoraro, M. Goussot, D. Bouchez, et al. 2010. The function of TONNEAU1 in moss reveals ancient mechanisms of

division plane specification and cell elongation in land plants. Development 137: p2733-p2742.

van der Knaap, E., M. Chakrabarti, Y.H. Chu, J.P. Clevenger, E. Illa-Berenguer, Z. Huang, et al. 2014. What lies beyond the eye: The molecular mechanisms regulating tomato fruit weight and shape. Frontiers In Plant Science 5: 227-227. doi:10.3389/fpls.2014.00227.

van der Knaap, E. and L. Østergaard. 2017. Shaping a fruit: Developmental pathways that impact growth patterns. Seminars in Cell and Developmental Biology. doi:10.1016/j.semcdb.2017.10.028.

Wang, S., Y. Chang, J. Guo and J.-G. Chen. 2007. Arabidopsis Ovate Family Protein 1 is a transcriptional repressor that suppresses cell elongation. The Plant Journal: For Cell And Molecular Biology 50: 858-872.

Wang, S., Y. Chang, J. Guo, Q. Zeng, B.E. Ellis and J.-G. Chen. 2011. Arabidopsis Ovate Family Proteins, a novel transcriptional repressor family, control multiple aspects of plant growth and development. PLoS ONE 6: 1.

Wang, Y.-K., W.-C. Chang, P.-F. Liu, M.-K. Hsiao, C.-T. Lin, S.-M. Lin, et al. 2010. Ovate family protein 1 as a plant Ku70 interacting protein involving in DNA double-strand break repair. Plant Molecular Biology 74: 453-466. doi:10.1007/s11103-010-9685-5.

Welty, N., C. Radovich, T. Meulia and E. van der Knaap. 2007. Inflorescence development in two tomato species. Canadian Journal of Botany 85: 111. doi:10.1139/B06-154.

Wu, S., B. Zhang, N. Keyhaninejad, G.R. Rodríguez, H.J. Kim, M. Chakrabarti, et al. 2018. A common genetic mechanism underlies morphological diversity in fruits and other plant organs. Nature Communications 9: 4734. doi:10.1038/s41467-018-07216-8.

Xiao, H., C. Radovich, N. Welty, J. Hsu, L. Dongmei, T. Meulia, et al. 2009. Integration of tomato reproductive developmental landmarks and expression profiles, and the effect of SUN on fruit shape. BMC Plant Biology 9: 1-21. doi:10.1186/1471-2229-9-49.

Yang, C., W. Shen, Y. He, Z. Tian and J. Li. 2016. OVATE Family Protein 8 positively mediates brassinosteroid signaling through interacting with the GSK3-like kinase in rice. Plos Genetics 12: e1006118-e1006118. doi:10.1371/journal.pgen.1006118.

Yu, H., W.Z. Jiang, Q. Liu, H. Zhang, M.X. Piao, Z.D. Chen, et al. 2015. Expression pattern and subcellular localization of the Ovate protein family in rice. PLOS ONE.

APPENDIX A

POTENTIAL CELL WALL INSTABILITY IN *ovate/sov1* BUDS

The bud clearing protocol described in Chapter 3 was usually very effective. However, some buds imaged would have a damaged or split interior. During the bud clearing process, the buds would be agitated in different solutions, and it is likely the buds were damaged during this step. Damage was usually minor for all accessions and badly damaged buds were not counted.

When the first inflorescence of Experiment 3 was examined, almost all the buds collected for *ovate/sov1* were broken apart (Figure A1). The other accessions had some splits in the bud interior and could still be used, but the broken buds of *ovate/sov1* were too destroyed to be of any use. All the accessions were treated the same during the bud clearing protocol. In Experiment 1 the first inflorescences from seedlings were used, but badly broken buds were not observed. However, the Experiment 3 was conducted at a different time of the year. The *ovate/sov1* plants in general display several physiological problems; these plants grew more slowly than the wild type or *ovate/sov1/trm5* and were harder to pollinate successfully. From the bud damage observed in the first inflorescence of Experiment 3 it seems possible that the *ovate/sov1* plants also have weaker bonding between their cell walls in these young buds. Further experiments are needed to test this theory.

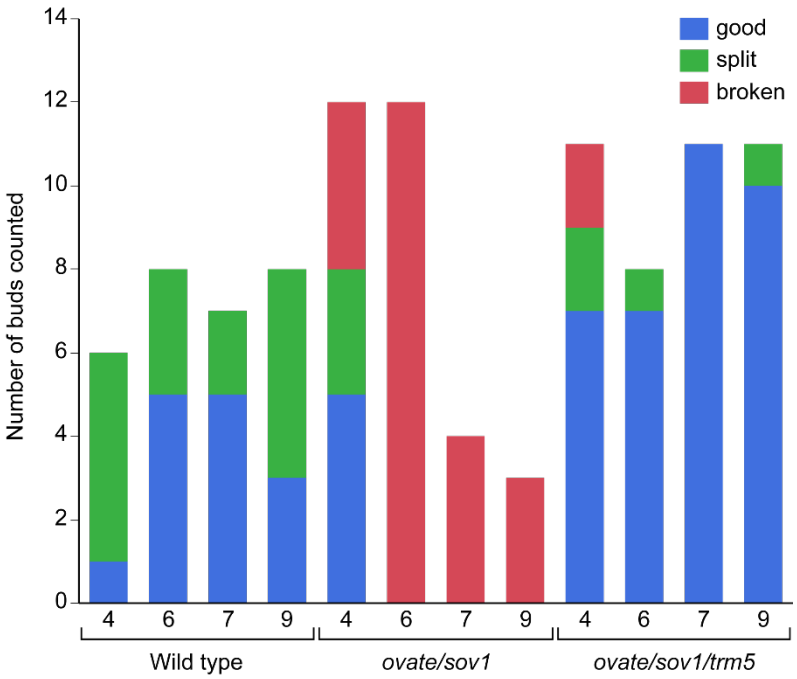

Figure A1. Number of damaged buds for different accessions. Buds at 4, 6, 7, and 9 days post initiation (dpi) imaged from the first inflorescence of Experiment 3 were scored visually as good, split, or broken.

APPENDIX B

INTERACTIONS OF THE FRUIT SHAPE GENE *sun* WITH *ovate*, *sov1*, AND *trm5*

The gene *SUN* affects tomato fruit shape, primarily after anthesis (van der Knaap et al., 2004, van der Knaap et al., 2014). This gene encodes a putative IQD family calmodulin-binding protein that interacts with the microtubules (Xiao et al., 2008; Bürstenbinder et al., 2017). The mutation *sun* is caused by a duplication of *SUN* from chromosome 10 to chromosome 7 (Jiang et al., 2009).

The *ovate/sov1* and *ovate/sov1/trm5* accessions were crossed with the *sun* mutant line in the LA1589 background. The purpose of this cross was to obtain three new nearly isogenic lines (NILs): *sun/trm5*, *ovate/sov1/sun*, and *ovate/sov1/sun/trm5*. The F1s from *ovate/sov1* and *ovate/sov1/trm5* by wild type LA1589 were selfed to obtain the F2. The progeny of four of these plants (18S280 and 18S281: WT x *ovate/sov1/trm5*; 18S282 and 18S283: WT x *ovate/sov1*) were planted in 96 well trays. DNA was extracted from the young seedlings using the DNA extraction for GenoGrinder protocol. The plants were genotyped for OVATE using the KASP primers 16EP19/16EP20/16EP/21 and PCR primers 12EP199/EP200. They were genotyped for SOV1 using PCR primers 13EP549/550/551. The plants were genotyped for SUN using the PCR markers EP2254/EP2255. They were genotyped for TRM5 using KASP markers 17EP3/17EP4/17EP5. Plants with the most fixed loci were selected to be selfed. One, 18S283-71, was already homozygous for *ovate/sov1/sun*, and the other plants were heterozygous for a few loci (Table B1).

Genotyping in the F3 generation identified four plants of the genotype *ovate/sov1/sun/trm5*, three of *sun/trm5*, and four of *ovate/sov1/sun* (Table B1). These plants were grown in the greenhouse with wild type LA1589.

Table B1. Plants selected in the F2 and F3 generations. F3 plants were used for fruit and leaf shape analysis and seeds were collected for future use. 1=derived allele, 2=heterozygote, 3=wild type allele.

Plant	*ovate*	*sov1*	*sun*	*trm5*
F2 plants selfed for homozygosity				
18S280-40	1	1	1	2
18S281-79	3	2	2	1
18S283-71	1	1	1	3
F3: *ovate/sov1/sun/trm5*				
18S388-4	1	1	1	1
18S388-7	1	1	1	1
18S388-8	1	1	1	1
18S388-9	1	1	1	1
F3: *trm5/sun*				
18S389-7	3	3	1	1
18S389-11	3	3	1	1
18S389-20	3	3	1	1
F3: *ovate/sov1/sun*				
18S390-2	1	1	1	3
18S390-3	1	1	1	3
18S390-5	1	1	1	3
18S390-6	1	1	1	3

Terminal leaflets were collected after the first inflorescence had flowered. From each plant, 4-6 leaflets were collected from below the inflorescence and stored on ice. The plants had bad edema, which affected the number of leaves that could be collected. The shape index (ratio of maximum height to maximum width) of leaves from these

plants were scanned and evaluated using Tomato Analyzer (Brewer et al., 2006). The *ovate/sov1/sun* plants had a significantly larger leaf shape index than the wild type, *ovate/sov1/sun/trm5*, and *sun/trm5* accessions when analyzed with a Student's t-test (Figure B1).

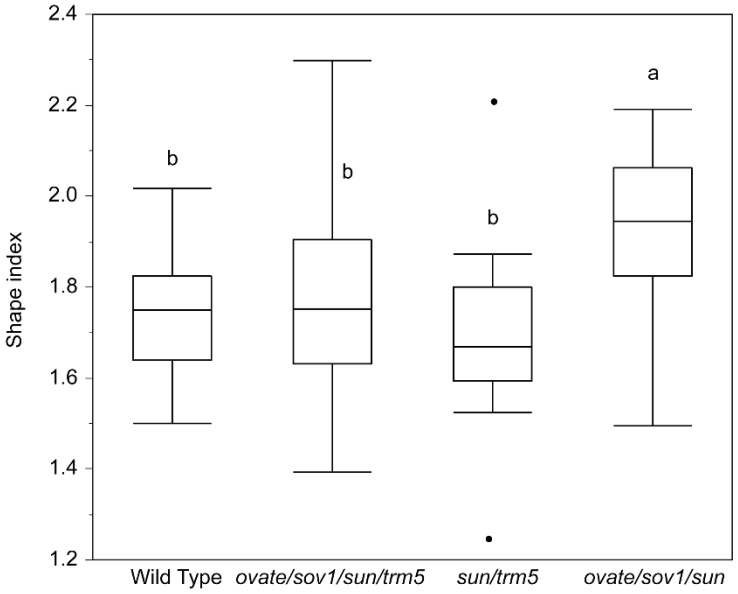

Figure B1. Leaf shape of terminal leaflet. 4-6 leaflets were used per plant, and 3-4 plants per accession were used. Shape index is the ratio of maximum height to maximum width, measured with Tomato Analyzer.

Fruits were collected when they were semi-ripe (orange color). Fruits were cut in half and scanned, then evaluated using Tomato Analyzer (Brewer et al., 2006). The shape index (ratio of maximum height to maximum width) of each accession was significantly different from all the others, as analyzed with a Student's t-test. The *ovate/sov1/sun* plants had a significantly larger fruit shape index than *ovate/sov1/sun/trm5*, followed by *sun/trm5*, and the wild type had the smallest shape

index (Figure B2). These results are preliminary; for a more comprehensive analysis these plants should be grown with the *sun* NIL as a control as well as the heterozygous plants.

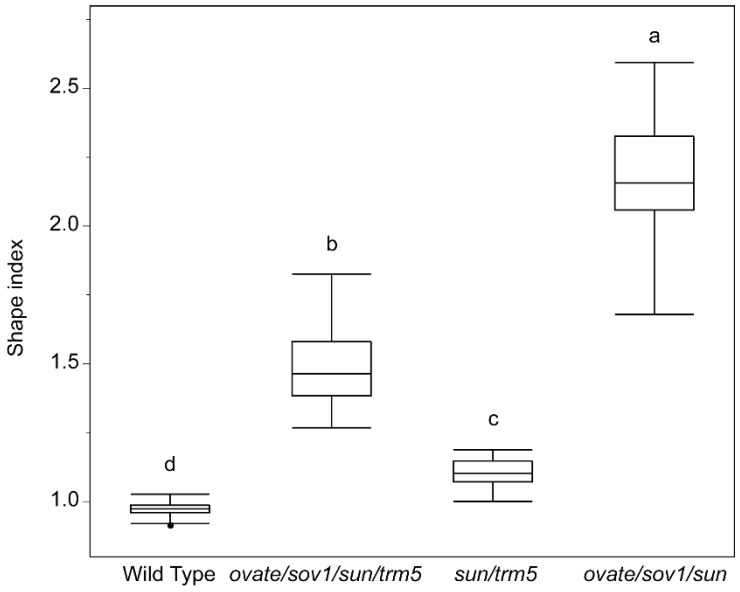

Figure B2. Fruit shape index of new NILs with *sun* compared to wild type LA1589. Shape index is the ratio of maximum height to maximum width, measured with Tomato Analyzer. Fruits from 3-4 plants per accession were used; fruit number wild type n=107, *ovate/sov1/sun/trm5* n=41, *sun/trm5* n=35, *ovate/sov1/sun* n=60.

APPENDIX REFERENCES

Brewer, M.T., L. Lang, K. Fujimura, N. Dujmovic, S. Gray and E. van der Knaap. 2006. Development of a controlled vocabulary and software application to analyze fruit shape variation in tomato and other plant species. Plant Physiol 141: 15-25. doi:10.1104/pp.106.077867.

Bürstenbinder, K., B. Möller, R. Plötner, G. Stamm, G. Hause, D. Mitra, et al. 2017. The IQD Family of Calmodulin-Binding Proteins Links Calcium Signaling to Microtubules, Membrane Subdomains, and the Nucleus. Plant Physiology 173: 1692-1708. doi:10.1104/pp.16.01743.

Jiang, N., D. Gao, H. Xiao and E. van der Knaap. 2009. Genome organization of the tomato sun locus and characterization of the unusual retrotransposon Rider. The Plant Journal 60: 181-193. doi:10.1111/j.1365-313X.2009.03946.x.

van der Knaap, E., M. Chakrabarti, Y.H. Chu, J.P. Clevenger, E. Illa-Berenguer, Z. Huang, et al. 2014. What lies beyond the eye: The molecular mechanisms regulating tomato fruit weight and shape. Frontiers In Plant Science 5: 227-227. doi:10.3389/fpls.2014.00227.

van der Knaap, E., A. Sanyal, S.A. Jackson and S.D. Tanksley. 2004. High-resolution fine mapping and fluorescence in situ hybridization analysis of sun, a locus controlling tomato fruit shape, reveals a region of the tomato genome prone to DNA rearrangements. Genetics 168: 2127-2140. doi:10.1534/genetics.104.031013.

Xiao, H., N. Jiang, E. Schaffner, E.J. Stockinger and E. van der Knaap. 2008. A retrotransposon-mediated gene duplication underlies morphological variation of tomato fruit. Science 319: 1527-1530. doi:10.1126/science.1153040.